62
Obinutuzumab (Gazyva®), a Novel Glycoengineered Type II CD20 Antibody for the Treatment of Chronic Lymphocytic Leukemia and Non-Hodgkin's Lymphoma

Christian Klein, Marina Bacac, Pablo Umaña, and Michael Wenger

62.1
In vitro Mechanism of Action of Type I and Type II CD20 Antibodies

CD20 is a transmembrane antigen expressed on the surface of malignant and non-malignant pre- and mature B-lymphocytes, but not on hematopoietic stem cells, pro-B cells, normal plasma cells, or other normal tissues [1, 2]. CD20 is believed to exist predominantly as a tetramer on cell surface and not to be subjected to shedding or internalization upon antibody binding. The physiological role of CD20 has not been clearly elucidated as yet, although it was suggested that it could be involved in calcium signaling following B-cell receptor activation [1, 2].

Rituximab (MabThera/Rituxan) was the first monoclonal antibody to be approved for the treatment of non-Hodgkin's lymphoma (NHL) including indolent non-Hodgkin's lymphoma (iNHL), diffuse large B-cell lymphoma (DLBCL), and chronic lymphocytic leukemia (CLL) in combination with chemotherapy. Recently, the human CD20 antibody ofatumumab (Arzerra) was approved for a subpopulation of fludarabine-refractory CLL patients [3].

Although the exact mechanism of action of rituximab remains to be fully elucidated, it is thought that CD20 antibodies trigger at least three different mechanisms of action: (i) cell death induction (also described as direct cell death or apoptosis), (ii) antibody-dependent cellular cytotoxicity (ADCC) and/or antibody-dependent cellular phagocytosis (ADCP), and (iii) complement-dependent cytotoxicity (CDC). The relative contribution of these mechanisms to the overall efficacy of rituximab is not clear; however, ADCC/ADCP are considered as the most important mechanisms of action of rituximab in patients, with CDC and induction of cell death playing a less important role [4, 5]. In the clinical setting, CD20 antibodies have been shown to work synergistically in combination with chemotherapy [2, 6]. Furthermore, the induction of an adaptive immune response following therapy with rituximab, also termed *vaccinal effect*, is currently being discussed [2, 7].

Obinutuzumab (also known as *GA101*, *RO5072759* or GAZYVA) is a humanized glycoengineered Type II CD20 monoclonal antibody of the immunoglobulin G1 (IgG1) isotype. Obinutuzumab was designed to mediate enhanced direct and immune effector-cell-mediated killing of tumor cells compared to the Type I CD20

Handbook of Therapeutic Antibodies, Second Edition. Edited by Stefan Dübel and Janice M. Reichert.

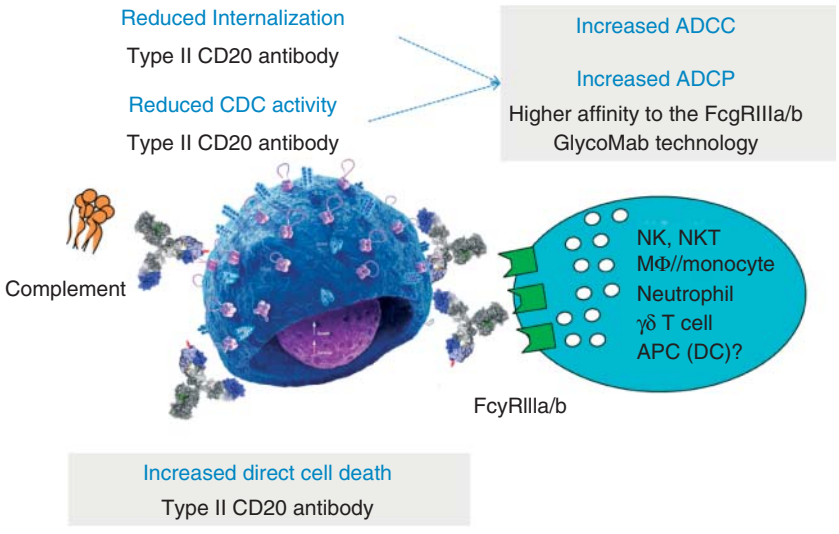

Figure 62.1 Putative mechanism of action of obinutuzumab compared to rituximab. ADCC, antibody-dependent cell-mediated cytotoxicity; ADCP, antibody-dependent cellular phagocytosis; APC, antigen-presenting cells; NK, natural killer; NKT, natural killer T cells.

antibody rituximab (Figure 62.1). It was derived by humanization and elbow-hinge optimization of the parental B-Ly1 mouse antibody and is further characterized by a glycoengineered Fc part to enhance its ADCC activity [8].

CD20 antibodies can be categorized as Type I or Type II CD20 antibodies (see Table 62.1) [9–16]. The majority of CD20 antibodies, including rituximab, ofatumumab, veltuzumab, ocaratuzumab or ocrelizumab, are categorized as Type I: Type I CD20 antibodies induce CD20 translocation into lipid rafts upon antibody binding. Clustering in lipid rafts is believed to foster recruitment and subsequent activation of complement; thus, Type I CD20 antibodies are potent inducers of CDC. In contrast, the two Type II CD20 antibodies obinutuzumab and B1 (tositumomab) do not induce CD20 clustering in the lipid rafts and, subsequently, mediate only low CDC activity [17]. Probably the most striking characteristic of Type I CD20 antibodies is that B cells accommodate twice the amount of Type I CD20 antibodies as compared to Type II CD20 antibodies [17, 18]. We and others have hypothesized that this may be due to differences in CD20 binding geometry [19] resulting in binding between two CD20 tetramers (inter-tetramer binding) for Type I CD20 antibodies, for example, cross-linking tetramers with two antibodies bound per tetramer, as opposed to Type II CD20 antibodies that bind within one tetramer (intra-tetramer binding), resulting in only one antibody bound per CD20 tetramer [11, 16]. Furthermore, Type II antibodies are more potent than Type I antibodies in inducing homotypic aggregation and direct cell death [18]. Recent studies have demonstrated that this is a nonapoptotic form of lysosomal cell death that is actin dependent and involves the generation of reactive oxygen

Table 62.1 CD20 antibodies can be categorized as type I or type II CD20 antibodies.

Type I	Type II
Localize CD20 to lipid rafts	Do not localize CD20 to lipid rafts
High CDC	Low CDC
ADCC activity	ADCC activity
Full binding capacity	Half binding capacity
Weak homotypic aggregation	Strong homotypic aggregation
Low cell death induction	Enhanced cell death induction
CD20 downmodulation (FcγRIIb mediated)	No CD20 downmodulation
Rituximab	Obinutuzumab
Ocrelizumab	Tositumomab
Ofatumumab	—

Type I/type II classification of CD20 antibodies according to mode of CD20 binding and primary mechanism of killing of CD20-expressing B cells.
Source: Taken from [16].

species (ROS) but does not show the classical hallmarks of apoptosis [20–22]. The ADCC and ADCP activity of CD20 antibodies is mediated by the interaction of their Fc regions with FcγRIIIa and not impacted by the Type I or Type II character of the antibody. However, it was recently shown that binding of Type II CD20 antibodies obinutuzumab and tositumomab does not result in internalization or downmodulation of CD20, whereas the Type I CD20 antibodies rituximab and ofatumumab result in FcγRIIb-mediated CD20 internalization on NHL samples [23, 24]. We have recently hypothesized that Type I antibodies may bind to CD20 in a manner that fosters simultaneous binding to FcγRIIb in cis and as a consequence cross-linking and signaling followed by CD20 and FcγRIIb internalization within lipid rafts. On the contrary, Type II antibodies such as obinutuzumab may show reduced internalization as they may bind in a different way so that the Fc portion cannot interact simultaneously with FcγRIIb [16] (Figure 62.2).

62.2 Generation of Obinutuzumab

Obinutuzumab was derived by humanization of the parental murine IgG1-κ antibody B-Ly1 that was for a long time known as a reagent for flow cytometry [8, 25]. B-Ly1 induces homotypic aggregation, as known for Type II antibodies, but does not stabilize CD20 in lipid rafts. Variable heavy (V_H) and light (V_L) chain regions were cloned from the B-Ly1 hybridoma, and the complementarity determining regions (CDRs) were grafted onto human V_H and V_L frameworks [8]. During this process, different human framework sequences were applied. CDR-grafted variants with identity to human germline V_H and V_L framework sequences and retained binding to CD20 were analyzed for their ability to induce

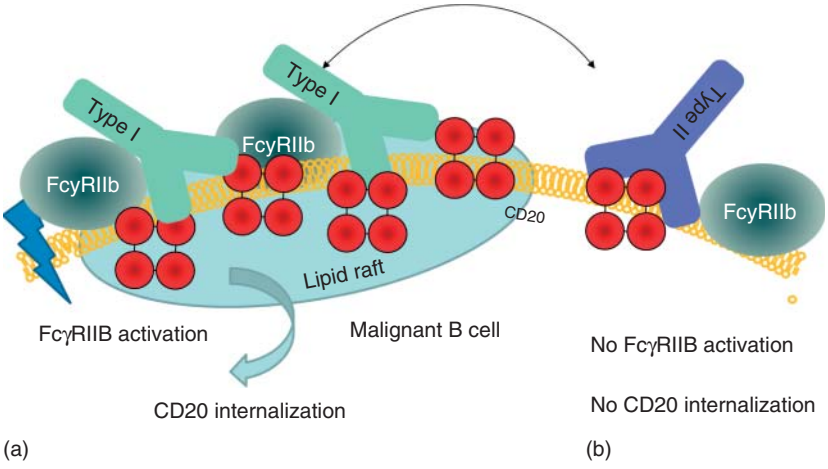

Figure 62.2 Hypothetical model for CD20 binding of type I and type II CD20 antibodies explaining the impact of FcγRIIb on internalization. (a) Type I antibodies, such as rituximab, may bind to CD20 in a conformation that allows simultaneous binding to FcγRIIb and subsequent cross-linking and activation followed by internalization in lipid rafts. (b) Type II antibodies, such as obinutuzumab, may bind in a conformation that does not allow simultaneous binding to FcγRIIb, thus resulting in low/no internalization. (Source: Taken from [16].)

direct cell death of human B-cell lymphoma *in vitro* using the annexin V/PI (propidium iodide) assay [8]. During this process, several variants were identified, which showed significantly enhanced direct cell death induction as compared to the parental murine B-Ly1 antibody. Surprisingly, the difference between variants inducing a strong versus weak cell death was one sequence alteration in the framework 1 region that is known as the so-called "elbow-hinge region." The elbow-hinge region is the region between the variable region and the first constant domain in the Fab fragment and affects the flexibility and angle of the Fab domains [26]. In particular, the presence of the valine-11 residue turned out to determine the Type II character of the respective humanized antibody's activity instead of the leucine-11 present in the murine original antibody [8]. On the basis of this finding, the process resulting in the discovery of obinutuzumab has been termed as *elbow-hinge engineering*, although it only involves introduction of one single residue naturally occurring in the elbow-hinge region of the antibody framework.

62.3 Obinutuzumab is a Classical Type II CD20 Antibody

On the basis of the number of properties mentioned above, CD20 antibodies can be characterized as Type I or Type II CD20 antibodies (see Table 62.1). Type I antibodies work primarily through ADCC and CDC, whereas Type II antibodies work through direct cell death and ADCC induction but mediate low

CDC activity. Obinutuzumab exhibits characteristics typical of a Type II CD20 antibody [8, 27]: at saturating antibody concentrations, obinutuzumab binds to cell surface of a panel of NHL cell lines at levels approximately one-half those of rituximab and ofatumumab [8, 27]. Unlike obinutuzumab, rituximab stabilizes CD20 molecules into Triton X-100-resistant lipid rafts on surface of B-cells, resulting in the distribution of CD20 into Triton X-100-insoluble pellet fraction whereas obinutuzumab does not mobilize CD20 into lipid rafts [8]. In fluorescence colocalization experiments, rituximab colocalizes with cholera toxin B (a lipid raft marker), whereas obinutuzumab does not [8]. Antibody–CD20 complexes in lipid rafts are believed to bind more strongly to C1q (the first subcomponent of the C1 complex of the classical pathway of complement activation), leading to higher levels of CDC compared with Type II antibodies. As a consequence, obinutuzumab displays reduced CDC relative to rituximab and ofatumumab [8, 27], in particular when physiological levels of human immunoglobulins are present [8]. However, obinutuzumab induces stronger homotypic aggregation of B cells *in vitro* compared to rituximab and results in superior induction of direct cell death on a panel of NHL cell lines compared to rituximab [8]. Mutating the elbow-hinge valine of obinutuzumab back to the parental murine leucine residue switches the cell death induction on and off [8] and results in partial loss of Type II characteristics, as seen by increased maximal binding to B cells, higher CDC activity, and reduced homotypic B-cell aggregation (E. Moessner, P. Umana).

62.4
The Epitope Recognized by Obinutuzumab

Obinutuzumab binds with single digit nanomolar affinity to CD20 expressed on malignant and nonmalignant B cells. The binding affinity (K_D value) of obinutuzumab for human CD20 on cells was determined to be approximately 4.0 nM by Scatchard analysis using SU-DHL-4 NHL cells and fluorescently labeled obinutuzumab, whereas a K_D value of approximately 4.5 nM was obtained for rituximab [8]. Experiments using obinutuzumab IgG, Fab2, and Fab fragments confirm that obinutuzumab binds in a bivalent manner through both arms to CD20 on cells, indicating that avidity and bivalent binding are required for its action (S. Herter, M. Bacac, C. Klein). Furthermore, binding experiments on cells using fluorescently labeled antibodies revealed that obinutuzumab, rituximab as well as ofatumumab compete with each other for binding to CD20 and thus recognize distinct but partially overlapping epitopes [27] (Figure 62.3).

Using Pepscan technology, site-directed mutagenesis, X-ray crystallography, surface plasmon resonance, and isothermal titration calorimetry, the binding properties and the epitope of obinutuzumab were investigated to compare the molecular interactions of obinutuzumab and B1 (tositumomab), the Type II antibodies, and rituximab and LT20, the Type I antibodies [16, 19]. Positional mapping confirmed that the epitopes of obinutuzumab and rituximab overlap. However, obinutuzumab's epitope is shifted toward the C-terminus of CD20 so

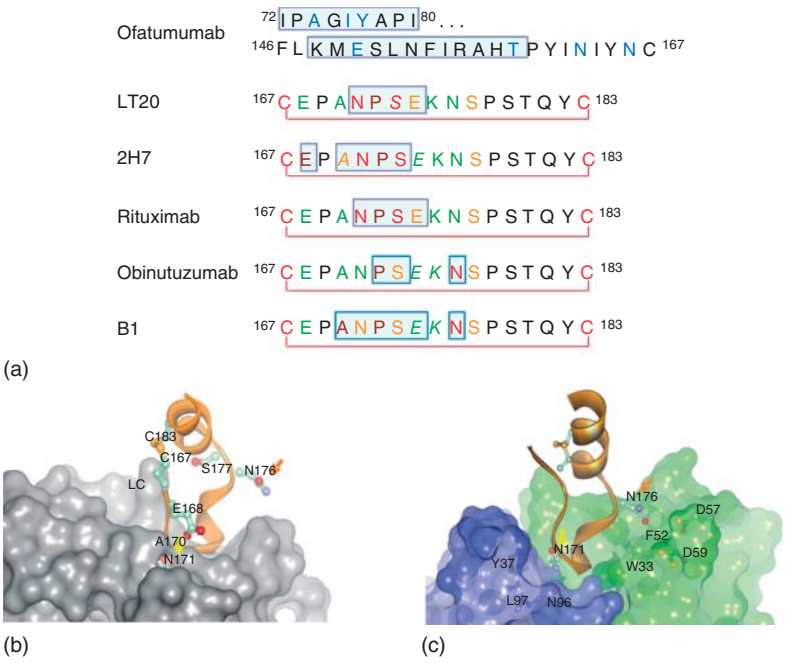

Figure 62.3 Type II epitope recognized by obinutuzumab and crystal structure of obinutuzumab in complex with cyclic CD20 peptide. (a) Sequence alignment of CD20 epitopes recognized by CD20 antibodies based on published information. Core epitope residues are boxed in light blue. For ofatumumab (2F2), core epitope assignment is based on published work [28, 29]. For residues labeled in blue, experimental evidence suggests a role in ofatumumab binding. For the other antibodies, the following coloring scheme has been applied based on Pepscan results and FACS binding data of amino acid exchange mutants: green, almost any exchange tolerated at this position; brown, non conservative exchange tested and not tolerated at this position; orange, conservative exchange tested and tolerated at this position; red, also conservative exchanges not tolerated at this position; black, position has not yet been evaluated. Italic font indicates that Pepscan and FACS binding results are discordant. As the FACS binding results better reflect the native protein context, the coloring in such instants was based on the FACS binding data. (b) Comparison of rituximab and (c) obinutuzumab crystal structures in complex with a cyclic CD20 peptide. While for rituximab N171 is deeply immersed and N176 has no contacts with the rituximab CDRs, N171 is not deeply immersed in the obinutuzumab CDRs and vice versa N176 makes contacts to residues F52/D57/D59 of obinutuzumab supporting the C-terminal shift of the obinutuzumab epitope. It is proposed that the differences in epitope recognition and binding geometry form the structural basis for the type II character of obinutuzumab. (Source: Modified from [16].)

that N176 is essential for binding of obinutuzumab, but not of rituximab. The core of the obinutuzumab epitope consists of residues 170-ANPSEKNSP-178, whereas rituximab relies on the 170-ANPS-173 stretch [30]. The obinutuzumab epitope determined by Pepscan technology was confirmed by crystallography. While the crystal structure shows that the N-171 residue in the ANP stretch is essential

for binding of rituximab, the same residue does form hydrogen bonds with obinutuzumab, but is not essential for its binding. The surrounding residues P-172 and S-173, however, contribute to the binding of obinutuzumab, and the residues at position 174–176 (174-EKN-176) form an extensive hydrogen bond network with the obinutuzumab CDRs. Overall, in the obinutuzumab–CD20 complex a larger covered surface area can be observed. Moreover, obinutuzumab binds CD20 in a different angle compared with rituximab and 2H7 (the murine parental antibody of ocrelizumab), as a consequence of both its unique epitope and the different elbow angle [16]. Rituximab and 2H7 bind to CD20 in positions oriented toward the core of the epitope [28]. In contrast, obinutuzumab is rotated 90° clockwise around its middle axis and tilted about 70° toward the C-terminus of the peptide (Figure 62.3). This difference in topology may in part explain several differences in the nonclinical and clinical activity observed between obinutuzumab and rituximab including differences in FcγRIIb-mediated internalization (see above) [16] (Figure 62.3). In line with this, confocal microscopy and protein tomography analysis suggest that CD20 molecules bound by Type I and Type II anti-CD20 antibodies, rituximab, and obinutuzumab, respectively, may differ in their localization and conformation [19].

62.5 CDC Activity of Obinutuzumab

Complement activation by obinutuzumab was tested in comparison to rituximab in different NHL cell lines having different CD20 expression levels, complement resistance, and growth properties (S. Herter, R. Grau). Depending on the assay conditions, obinutuzumab mediated a >100-fold decreased potency of CDC induction in comparison to rituximab [8]. In particular, while the CDC activity of rituximab was almost not influenced by addition of physiological concentrations of human nonspecific IgG, the CDC activity of obinutuzumab was almost completely abolished. However, obinutuzumab was still able to mediate CDC at very high saturating concentrations [8]. When obinutuzumab was compared with rituximab and ofatumumab for CDC activity on Z138 and SU-DHL-4 cell lines, the reduced CDC activity was confirmed [27]. *In vivo* xenograft studies in the RL model using cobra venom toxin as complement inhibitor demonstrated that in contrast to rituximab CDC does not seem to contribute to the anti-tumoral efficacy of obinutuzumab (105).

In addition to cellular studies, biochemical experiments with isolated C1q indicate that obinutuzumab has a diminished binding capacity for C1q compared to rituximab [31] and ofatumumab [27]. Recently, Weiner and colleagues showed that the recruitment of the complement factor C3b can interfere with natural killer (NK) cell activation and ADCC function of rituximab by steric hindrance [32]. Similar experiments with obinutuzumab showed that while complement in serum blocked NK activation induced by rituximab, it had no effect on NK cell activation induced by obinutuzumab. Similarly, complement blocked rituximab-induced NK-cell-mediated ADCC, but not obinutuzumab-induced NK-cell-mediated ADCC [31]. These results demonstrate that the decreased ability of obinutuzumab to fix

complement relative to rituximab may actually result in an enhanced ability of obinutuzumab to recruit and activate NK cells when serum is present. Thus, the decreased ability of obinutuzumab to fix complement could, paradoxically, further enhance the ADCC-dependent efficacy of obinutuzumab [31].

In conclusion, these data support the notion that obinutuzumab, relative to rituximab and ofatumumab, has significantly reduced CDC activity, both in terms of efficacy and potency. It is difficult to predict whether under the physiological concentrations as they occur in CLL and NHL patients, CDC may contribute significantly to the mechanism of action of obinutuzumab, however the Phase 1 clinical data did not show any evidence of complement activation in patients treated with obinutuzumab (106). As the contribution of CDC to the mechanism of action of rituximab is controversial, it is currently assumed that CDC does not play a major role in the efficacy of obinutuzumab [9–15].

62.6 Direct Cell Death Induction by Obinutuzumab

CD20 has been shown to play a role during B-cell cycle progression [33, 34], and CD20 antibodies, such as rituximab, can inhibit NHL tumor cell proliferation and induce apoptosis and/or nonclassical cell death in NHL cell lines [35–48]. Antibody-mediated direct cell death induction has also been described for antibodies against other lymphocyte antigens, including HLA-DR [49], CD47 [50, 51], CD37 [52, 53], CD99 [54–56], and others. However, the molecular mechanism of cell death induction mediated by these antibodies, whether through apoptosis or nonapoptotic cell death, is still controversial.

It has been shown that the murine Type II CD20 antibody B1 (tositumomab) mediates superior induction of apoptosis or cell death in comparison to Type I antibodies [18, 57]. Likewise, obinutuzumab induces dose-dependent and rapid onset of surface exposure of phosphatidylserine accompanied by concomitant cell death, as measured by Annexin V binding and appearance of Annexin V/PI double-positive cells [8]. The superior ability of obinutuzumab to induce direct cell death compared to rituximab was confirmed on a panel of NHL cell lines of different origin, including Burkitt's lymphoma (Raji, Ramos), mantle cell lymphoma (MCL) (Z138), DLBCL; cell lines of the activated B-cell-like (ABC) subtype (OCI-LY-10) and germinal center B-cell-like (GCB) (SU-DHL-4, WSU-DLCL-2) subtype. Cell death induction was detected by quantification of phosphatidylserine exposure (Annexin V binding) and propidium iodide (PI) staining [8]. When compared to B1 (tositumomab), the murine prototype Type II CD20 antibody that has demonstrated *in vitro* direct cell-death-inducing activity superior to rituximab obinutuzumab exhibited more pronounced direct cell death induction in Z138 MCL cells [8]. Similar results were obtained when obinutuzumab was compared to rituximab and ofatumumab for induction of direct cell death. Obinutuzumab was superior to rituximab and ofatumumab in inducing cell death of Raji, WIL2S, and Z138 NHL cells [27]. To rule out that cell death induction by obinutuzumab

is related to mechanical disruption during fluorescence-activated cell sorting (FACS) analysis [58–60], antibody-induced direct cell death was assessed using time-lapse confocal microscopy and Annexin V/PI labeling of CD20-expressing Z138 tumor cells. These studies revealed that obinutuzumab was superior to rituximab and ofatumumab in inducing direct cell death in the absence of any mechanical manipulation [27]. In addition, normal human peripheral blood B cells were sensitive to obinutuzumab when incubated in the absence of plasma and of immune effector cells *in vitro*. Interestingly, manipulation of the activation status of B cells using standard mitogens, including anti-immunoglobulin M (IgM) and anti-CD40 antibodies, resulted in increased sensitivity of B cells derived from human CD20 transgenic mice to obinutuzumab [8]. Further investigation into mechanisms implicated in direct cell death induction revealed that the process can be induced by the F(ab)′2 but not the Fab′ antibody fragment of obinutuzumab and it cannot be blocked by caspase inhibitors, supporting the view that it is a form of nonclassical apoptosis (Sylvia Herter, Georg Fertig). The detailed molecular mechanisms of cell death induction by Type II CD20 antibodies remain unresolved to date and are the subject of ongoing experimental investigation. Ivanov and colleagues [22] reported that the prototype Type II antibody B1 (tositumomab) and an HLA-DR antibody induce a novel form of lysosomal cell death that is elicited in a rapid nonapoptotic and nonautophagic manner and is dependent on the integrity of plasma membrane cholesterol and activation of the V-type ATPase. The cytoplasmic cell death involves lysosomes, which swell and disperse their contents, including cathepsin B into the cytoplasm and surrounding environment. The resulting loss of plasma membrane integrity occurs independently of caspases and is not controlled by Bcl-2 [22]. Furthermore, they demonstrated that obinutuzumab-induced cell death is dependent on actin reorganization and lysosome disruption, can be abrogated by inhibitors of actin polymerization, and is independent of BCL-2 overexpression and caspase activation [20]. In addition, cell death induction by obinutuzumab correlates with its ability to produce ROS in human B-lymphoma cell lines and primary B-cell chronic lymphocytic leukemia (B-CLL) cells. The addition of ROS scavengers abrogated cell death induction, indicating that ROS are required for the execution of cell death. ROS were generated downstream of antibody-induced actin cytoskeletal reorganization and lysosomal membrane permeabilization, and were independent of mitochondria and unaffected by Bcl-2 overexpression. Instead, ROS generation was mediated by nicotinamide adenine dinucleotide phosphate (NADPH) oxidase. These findings imply that NADPH-oxidase-derived ROS may be involved in mediating nonapoptotic direct cell death in B-cell malignancies [21]. Hallaert and colleagues had previously shown that *in vitro* CD40 stimulation of peripheral blood-derived CLL cells results in resistance to cytotoxic drugs [61]. In contrast to this, CD40 stimulation sensitizes CLL cells to cell death induction by obinutuzumab, overcoming CD40-induced resistance mechanisms [47, 62]. Cell death occurred without cross-linking and involved a lysosome-dependent mechanism. Furthermore, the combination of obinutuzumab with various cytotoxic drugs resulted in additive cell death, in CD40-stimulated CLL cells, and also in p53-dysfunctional

CLL cells. Lastly, it was shown that the cell death induced by obinutuzumab has features of immunogenic cell death induction characterized by the release of damage-associated molecular patterns (DAMPs), including HSP90, HMGB1, and adenosine triphosphate (ATP), which can induce dendritic cell maturation and subsequent T-cell proliferation. Thus, cell death induction by obinutuzumab may ultimately enhance host immune response and help induce durable tumor remissions [63].

62.7 Glycoengineering of Obinutuzumab

In addition to direct effects, the biological activity of therapeutic antibodies relies on the interaction between the antibody's Fc part and membrane-bound Fcγ receptors expressed on a variety of effector cells. The cross-linking of FcγRs triggers cellular immune responses including the release of cytokines, chemokines, and mediators that kill target cells (perforin and granzymes), resulting in ADCC and ADCP [64]. Fc receptors consist of an immunoglobulin-binding chain containing two immunoglobulin-like domains that form the extracellular region. There is one high-affinity IgG receptor in humans (hFcγRI, CD64), and two families of low-affinity IgG receptors – hFcγRIIA, IIB and IIC, CD32; and hFcγRIIIA and IIIB, CD16. hFcγRI and hFcγRIIIA are FcRγ-associated activating receptors, hFcγRIIA and hFcγRIIC are single-chain activating receptors, hFcγRIIB is a single-chain inhibitory receptor, and hFcγRIIIB is a GPI-anchored receptor expressed on human neutrophils [65]. Despite the affinity variations, the basic binding mode is similar to all members of the immunoglobulin-like Fcγ receptors as the sites of interaction between the activating and inhibitory Fcγ receptors and IgG are structurally conserved [64]. Posttranslational modifications, in particular the glycosylation of both antibodies and Fcγ receptors, modulate the affinity of interaction [66–75]. Glycosylation of the Fc region of human IgGs occurs at a conserved N-glycosylation site at asparagine 297 (Asn297) within the CH2 domain. Deglycosylated IgGs are almost completely devoid of Fc-mediated immune effector functions as a consequence of drastically reduced binding to FcγRs or to proteins of the complement system [76]. The lack of only one of the sugars, namely the fucose residue in an α1,6-linkage to the first *N*-actetylgucosamine (GlcNAc) of Fc-oligosaccharide core (''core fucosylation''), actually results in enhanced binding to FcγRIIIa,b [77] and enhanced effector functions mediated by this receptor [78].

Roche Pharmaceutical Research and Early Development, Zürich, has developed the so-called ''GlycoMab technology'' that enhances the binding affinity of therapeutic antibodies to the high- and low-affinity FcγRIIIa and FcγRIIIb by introduction of bisecting GlcNAc residue in the carbohydrate chain of the antibody Fc region. The introduction of GlcNAc results in steric interference and affects the core antibody fucosylation, resulting in the production of ''defucosylated'' or ''afucosylated'' antibodies [78–81], a process also known as *antibody glycoengineering* [82, 83] (Figure 62.4). Glycoengineering exclusively enhances the affinity of human

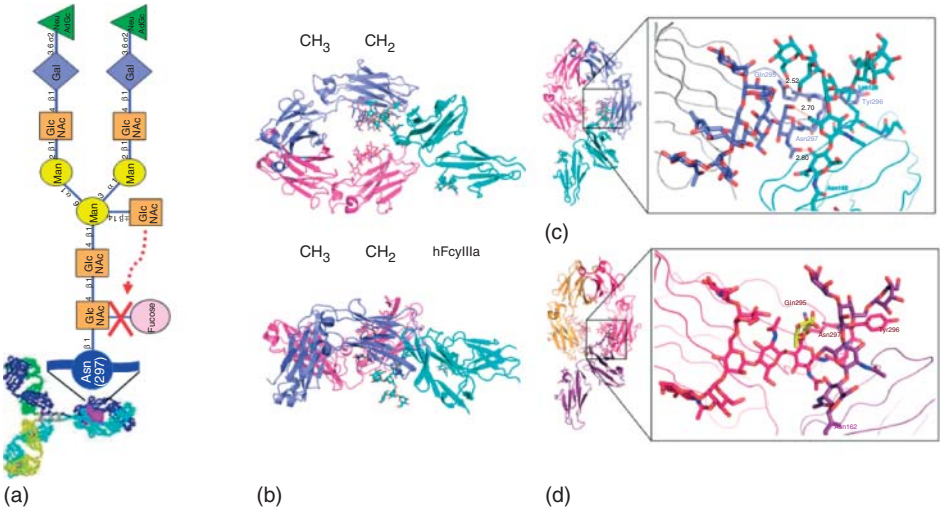

Figure 62.4 Carbohydrate of glycoengineered antibody and crystal structure of glycoengineered and nonglycoengineered Fc region with glycosylated FcγRIIIa extracellular domain. (a) Scheme of the glycoengineered, bisected carbohydrate chain of a glycoengineered antibody. Structure of glycosylated Fc/FcγRIIIa. (b) Top and side views of the structure of the glycosylated Fc/FcγRIIIa complex. The Fc chains are shown in blue and magenta, the receptor in cyan. The oligosaccharides are depicted as ball and stick representations. (c) View on the interaction interface between defucosylated Fc fragment and glycosylated Fc receptor. Chain A of the Fc fragment is shown in blue, the Fc receptor in cyan. Hydrogen bonds are presented as dashed lines with distance between donor and acceptor shown. (d) View on the interaction interface between fucosylated Fc fragment and glycosylated Fc receptor. Chain A of the Fc fragment is shown in magenta, the Fc receptor in dark violet. Core fucose of fucosylated Fc is highlighted in yellow. (Source: Modified from [70].)

IgG1 antibodies to human FcγRIIIa and FcγRIIIb and subsequently results in enhanced ADCC and ADCP [78, 80, 81]. In contrast to mutations in the Fc region that enhance the FcγRIII interaction, glycoengineering leaves the binding to other human activating and inhibitory receptors (FcγRIIA or FcγRIIB) largely unchanged, suggesting that despite the overall similarity in protein structure, individual FcγRs have unique binding patterns [70, 77, 84, 85]. The structural basis of the enhanced affinity of defucosylated Fc regions to FcγRIIIa was recently elucidated by X-ray crystallography and showed a characteristic carbohydrate interaction that is responsible for the enhanced affinity of afucosylated antibodies for FcγRIIIA as opposed to non-glycoengineered antibodies [70, 86] (Figure 62.4). As expected, based on the different interaction sites of the Fc region with Fcγ receptors and with FcRn, glycoengineering does not impact FcRn binding and does not affect the antibody's pharmacokinetic properties.

Mogamulizumab (Kyowa Hakko Kirin, Japan), a humanized glycoengineered defucosylated antibody against CCR4 [87, 88], is the first glycoengineered antibody that has been approved for patients with relapsed or refractory CCR4-positive adult

T-cell leukemia/lymphoma in Japan in 2012 [89–92] and is in PhII clinical trials in the United States and Europe. More than 10 additional glycoengineered and/or ADCC-enhanced antibodies are currently in clinical trials; of those, obinutuzumab is the most advanced in pivotal clinical trials and approved in the US [93].

Obinutuzumab is produced in Chinese hamster ovary (CHO) cells by coexpression with β1,4-*N*-acetylglucosaminyltransferase III (GnTIII) and Golgi α-mannosidase II (Man-II). Subsequently, the Fc region of obinutuzumab is glycoengineered resulting in bisected, defucosylated Fc region carbohydrates and a concomitant increase in the binding affinity to the FcγRIIIa and FcγRIIIb receptor. The affinity of antibodies with glycoengineered Fc regions was shown to be approximately 50-fold enhanced for the human high-affinity allele of the FcγRIIIa (V158) receptor and approximately 27-fold enhanced for the low-affinity allele of the FcγRIIIa (F158) receptor, using surface plasmon resonance [86]. The average K_D values of the glycoengineered antibody obinutuzumab are 55 and 270 nM, and for rituximab, the values are 660 nM and 2 μM for the high- and low-affinity FcγRIIIa receptor, respectively. In addition, glycoengineering does not affect binding to the inhibitory human FcγRIIb receptor [70, 86]. In summary, glycoengineering results in a significantly increased affinity of obinutuzumab for the low- and high-affinity human FcγRIIIa receptors in comparison to rituximab. Most importantly, binding affinity to the low-affinity FcγRIIIa receptor is substantially increased such that it exceeds that for the high-affinity receptor with rituximab.

The human glycosylphosphatidylinosotol (GPI) anchored FcγRIIIb is a low-affinity receptor involved in the removal of immune complexes from the circulation. FcγRIIIb is expressed on neutrophil granulocytes or polymorphonuclear neutrophils (PMNs) and is 96% conserved in the extracellular domain compared to FcγRIIIa [94]. Contrary to FcγRIIIa, it is not capable of mediating ADCC but believed to be involved in phagocytosis [95]. The FcγRIIIB interaction is sensitive to the antibody fucosylation state [96]. In line with these data, surface plasmon resonance showed that as a consequence of glycoengineering, obinutuzumab also has approximately 8-fold enhanced affinity for FcγRIIIb-NA2 as compared to non-glycoengineered wild-type rituximab [97].

62.8 *In vitro* NK Cell and Neutrophil ADCC and Macrophage ADCP Activity of Obinutuzumab

The enhanced affinity of obinutuzumab for the low- and high-affinity FcγRIIIa translates into a significantly enhanced ADCC potency in comparison to rituximab using different ADCC assay formats, independent of the genotype of the FcγRIIIa receptor (V158/V158, F158/F158, or F158/V158). Overall, obinutuzumab exhibits up to 35- to 100-fold enhanced ADCC potency compared to rituximab [8] and ofatumumab [27]. This broad range of improvement in ADCC potency is the consequence of assay variabilities, including donor-related factors, CD20 expression levels, and ADCC-assay-specific factors. Most importantly, obinutuzumab exhibits significant

ADCC in the presence of physiological concentrations of human nonspecific competing endogenous IgG, whereas the ADCC activity of rituximab is completely abolished under these circumstances [8]. As a consequence of ADCC, a strong upregulation of the NK cell activation marker CD107a occurs and a downregulation of surface FcγRIIIa expression is observed (Sylvia Herter, Christian Klein, Pablo Umana). Therefore, despite occupying only half the number of CD20 receptor binding sites on B and NHL cells, obinutuzumab achieves superior ADCC compared to rituximab and ofatumumab bearing a wild-type Fc part.

As described above, complement in serum blocked NK cell activation induced by rituximab, but had no effect on NK cell activation induced by obinutuzumab [31]. These results demonstrate that the decreased ability of obinutuzumab to fix complement relative to rituximab may actually result in an enhanced ability of obinutuzumab to recruit and activate NK cells when serum is present [31].

CD20 internalization following incubation with obinutuzumab as well as rituximab has not been observed on NHL cell lines. Recently, it was demonstrated that Type II CD20 antibodies, obinutuzumab and tositumomab, do result in low internalization or downmodulation of CD20 upon binding, whereas Type I CD20 antibodies, such as rituximab and ofatumumab, can actually result in FcγRIIb-mediated CD20 internalization on patient-derived NHL samples [23, 24]. Thus, the decreased ability of obinutuzumab to fix complement and the putative reduced internalization of obinutuzumab as a Type II antibody may further enhance the ADCC-dependent efficacy of obinutuzumab compared to Type I antibodies such as rituximab.

As FcγRIIIa is also expressed in γδ T cells, Braza and colleagues [98] checked the capability of obinutuzumab to mediate ADCC with γδ T cells. Their data show that obinutuzumab can recruit and activate γδ T cells for target cell killing through ADCC and is more efficacious than rituximab. The relevance of γδ T cells for the clinical mechanism of action of obinutuzumab still needs further investigation.

Pievani and colleagues [99] have shown that the enhanced ADCC mediated by obinutuzumab can be applied to enhance the killing potency of adoptive immunotherapy with cytokine-induced killer (CIK) cells and CD20 antibodies.

The capability of obinutuzumab to mediate ADCP was investigated using M1 and M2c macrophages generated from human monocyte-derived macrophages (MDM) in comparison to rituximab and ofatumumab [27]. These data showed that all three CD20 antibodies displayed comparable phagocytic activity. Similarly, Bologna and colleagues [100] showed comparable phagocytic activity of obinutuzumab and rituximab in CLL samples. Recent experiments pointed out that in the presence of physiological levels of nonspecific, competing, human IgGs (a situation that more closely mimics the natural setting), obinutuzumab more strongly engages monocytes and macrophages and leads to significantly higher elimination of CD20-expressing tumor cells as compared to rituximab and ofatumumab as shown by assays detecting total antibody activity (ADCP, ADCC, and direct effects). These data showed, for the first time, that in addition to enhancing FcγRIIIa-dependent NK-cell cytotoxicity (ADCC), glycoengineering also enhances monocyte and macrophage

phagocytic activities through enhanced binding to FcγRIIIa under conditions that more closely resemble the physiological setting [101].

Golay and colleagues investigated the functional activity of on human neutrophil granulocytes or polymorphonuclear neutrophiles (PMNs) in response to obinutuzumab compared to rituximab and a glycoengineered version of rituximab [102]. Obinutuzumab activated PMN more efficiently than rituximab leading to increased CD11b expression and a downmodulation of CD62L. The activation was not accompanied by generation of ROS or by FcγRIIIb-mediated ADCC. In contrast, activation of purified PMN resulted in phagocytosis of opsonised targets, which involved FcγRIIIb and lead to PMN death. Furthermore, significant phagocytosis could be observed in whole blood only in presence of glycoengineered antibodies, similarly to what is observed for NK cell activation and ADCC. These data imply that phagocytosis of opsonized targets by PMNs may be an additional mechanism of action for obinutuzumab. While FcγRIIIb cannot activate signaling events downstream of FcγRIIIb and cannot activate ADCC of PMNs, it may function as an adaptor to bind glycoengineered obinutuzumab on its surface resulting in recruitment of PMNs into the tumor, enhanced binding to CLL cells, and subsequently, tumor accumulation by avidity followed by engulfment through ADCP. The recruitment and activation of PMNs through FcγRIIIb may offer an explanation for the neutropenia observed in some CLL patients treated with obinutuzumab, an effect likely related to its anti-leukemia activity.

Owing to the expression of FcγRIIIa on antigen-presenting cells (APCs) and the enhanced affinity of obinutuzumab for this receptor, enhanced antigen presentation to T cells via FcγRIIIa-expressing APCs such as dendritic cells (DCs) may contribute to enhanced secondary immune responses induced by obinutuzumab as compared to non-glycoengineered wild-type antibodies. Whether this proposed further mechanism of action of obinutuzumab may contribute to its clinical efficacy is currently under investigation in fully immunocompetent preclinical models.

62.9 *Ex vivo* Whole Blood B-Cell Depletion by Obinutuzumab

Whole blood contains the natural effector cell populations, human complement, and physiological concentrations of human IgG and thus allows measuring the effects of ADCC- inducing, CDC- inducing, and direct cell-death-inducing mechanisms in a system that more closely reflects the *in vivo* situation in peripheral blood. In whole blood samples from a panel of 10 healthy donors, representing each of three FcγRIIIa genotypes (high-affinity [158V/158V], intermediate-affinity [158F/158V], and low-affinity [158F/158F] receptors), obinutuzumab was found to be approximately 10- to 25-fold more potent in terms of EC50 values and approximately 1.5- to 2.5-fold more efficacious in terms of absolute B-cell depletion in comparison to rituximab [103]. In a separate set of experiments obinutuzumab also showed superior whole blood B-cell depletion as compared to rituximab and ofatumumab [27]. Obinutuzumab maintained superior activity even in whole

blood samples treated with lepirudin (a thrombin-specific agent that does not interfere with complement activation) and in heat-inactivated blood samples confirming that mechanisms underlying its superior B-cell depletion are complement independent [27].

Superior whole blood B-cell depletion mediated by obinutuzumab as compared to rituximab was also shown in a number of studies using samples derived from CLL patients [8, 100, 103–106]. In whole blood isolated from B-CLL patients, obinutuzumab mediated superior B-cell depletion both in terms of potency and absolute efficacy in 8/11 patients in direct comparison to rituximab [103]. Mechanism of action studies pointed out that in B-CLL whole blood assays, NK-cell-mediated ADCC appears to be the most important factor contributing to B-cell depletion [100, 104–106]. In addition, IL-8 appeared to act as an endogenous NK coactivator for NKs 105]. Notably, obinutuzumab was highly effective against CLL cells *ex vivo*, irrespective of high-risk prognostic markers including complex karyotype (three or more chromosomal abnormalities), 17p deletion, and recurrent somatic mutations of the TP53, NOTCH1, and SF3B1 genes [107].

62.10
In vivo Activity of Obinutuzumab in Xenograft Models

The dose-dependent efficacy of obinutuzumab and its superiority over rituximab were demonstrated in the subcutaneous (s.c.) SU-DHL-4 DLBCL xenograft model [8]. Weekly dosing of rituximab at 1, 10, and 30 mg kg^{-1} (q7d × 3) in mice bearing established s.c. SU-DHL-4 tumors of an average size of 200 mm^3 resulted in slowdown of tumor progression. At 1 mg kg^{-1} dose level obinutuzumab led to tumor growth inhibition (TGI) of 36% and tumor control ratio (TCR) of 0.58 (confidence interval (CI) 0.43–0.84). The induction of tumor stasis occurred at a dose of 10 mg kg^{-1} corresponding to a TGI of 77% and a TCR of 0.58 (CI 0.43–0.84), whereas complete tumor remission with TGI >100% and TCR of 0 was achieved in all animals at a dose of 30 mg kg^{-1} resulting in long-term survival (cure) in 9 out of 10 treated animals. Trough serum levels for 1, 10, and 30 mg kg^{-1} corresponded to approximately 11, 109, and 312 μg ml^{-1} at study termination. In contrast, the maximal effect of rituximab was reached with 10 mg kg^{-1}, and an increase in dose to 30 mg kg^{-1} did not result in further enhancement of efficacy despite the trough serum level increasing from 57 to 185 μg ml^{-1}. At the maximal dose of 30 mg kg^{-1} rituximab could only slow down tumor progression but did not induce tumor remission. These nonclinical data demonstrate an outstanding dose-dependent antitumor activity of obinutuzumab in this aggressive NHL xenograft model that is clearly different from that of rituximab at saturating doses [8]. In order to investigate whether the enhanced efficacy of obinutuzumab is due to glycoengineering, an experiment using 30 mg kg^{-1} (q7d × 4, i.v. (intravenous)) of obinutuzumab and a non-glycoengineered, wild-type version of obinutuzumab in the s.c. SU-DHL-4 model was performed (Sabine Lang, Christian Gerdes). Notably, the non-glycoengineered wild-type version of obinutuzumab was able to induce

complete tumor remission similar to obinutuzumab at the same dose with only a slight delay in onset, whereas tumors treated with rituximab at the same dose showed only tumor growth inhibition (TGI). These data indicate that the superiority of obinutuzumab is not only due to glycoengineering but rather related to its Type II character as well. Subsequently, the single-agent efficacy of obinutuzumab, rituximab, and ofatumumab was compared in the SU-DHL-4 model [27]. All three antibodies were dosed at 30 mg kg^{-1} (q7d × 6, i.p.) in mice bearing large established s.c. SU-DHL-4 tumors. Assessment of the first-line TGI on day 46 after tumor cell inoculation demonstrated tumor regression (TGI 120%) with obinutuzumab, but only tumor stasis with rituximab and ofatumumab (100 or 106%, respectively) compared to vehicle control. The superiority of the treatment with obinutuzumab was also demonstrated by 7 out of 10 tumor-free animals at day 67, whereas treatment with rituximab or ofatumumab resulted in 4 out of 10 or 2 out of 10 tumor-free animals, respectively [27].

In order to mimic rituximab-refractory NHL, a study evaluating the efficacy of second-line obinutuzumab treatment against s.c. SU-DHL-4 xenografts progressing under first-line weekly rituximab treatment with a dose of 30 mg kg^{-1} was performed [8]. Animals were given 30 mg kg^{-1} rituximab (q7d × 2, i.v.) and were subsequently randomized when tumors reached an average size of 700 mm^3. Treatment of these advanced xenografts with weekly obinutuzumab at 30 mg kg^{-1} (q7d × 4, i.v.) as second-line treatment controlled tumor progression. In comparison, second-line rituximab-treated tumors were refractory and no longer responded to rituximab treatment [8]. Similarly, the efficacy of obinutuzumab, rituximab, and ofatumumab applied as second-line treatment was evaluated in the SU-DHL-4 model [27]. Mice bearing large established s.c. SU-DHL-4 tumors first received 10 mg /kg^{-1} of rituximab (q7d × 2, i.p.) before administration of obinutuzumab, rituximab, or ofatumumab at 30 mg kg^{-1} (q7d × 5, i.p.) or vehicle control. Second-line treatment with obinutuzumab, rituximab, and ofatumumab resulted in a TGI of 64, 20, and 26%, respectively, on day 64 compared to control with one animal from the obinutuzumab group achieving complete remission at day 63 [27].

In addition to the s.c. xenograft models, obinutuzumab was evaluated in the aggressive disseminated Z138 MCL model at weekly doses ranging from 10 to 30 mg kg^{-1} (q7d, i.v.). i.v. injection of Z138 cells into severe combined immunodeficiency (SCID) beige mice resulted in large intraperitoneal lymphoid tumors in the ovary. In this model, obinutuzumab mediated increased overall and median survival at doses of 10 mg kg^{-1} (q7d × 3, i.v.) compared to rituximab [8]. The duration of survival could be increased with weekly doses of 1–10 mg kg^{-1}; however, a further increase of dose to 30 mg kg^{-1} (q7d × 3, i.v.) did not result in a further increase of efficacy in this model (C. Gerdes).

Obinutuzumab and rituximab were also compared in the fast-growing s.c. transformed follicular RL xenograft model [108]. Both antibodies were given twice weekly, obinutuzumab at doses of 10, 30, and 100 mg kg^{-1} (q3d × 5, i.p.) and rituximab at a dose of 30 mg kg^{-1} (q3d × 5, i.p.). Obinutuzumab showed dose-related activity in terms of TGI, with TGI of 25, 75, and 85%, respectively. While the lowest dose of 10 mg kg^{-1} was ineffective, the higher doses of 30 and

Table 62.2 Obinutuzumab activity in NHL xenograft models.

Name	Origin	Route	Comment
SU-DHL-4	DLBCL (GCB)	s.c.	Superior to rituximab
WSU-DLCL-2	DLBCL (GCB)	s.c./i.v.	Superior to rituximab
Z138	MCL	s.c./i.v.	Superior to rituximab
RL	fNHL	s.c.	Superior to rituximab
OCI-LY18	DLBCL (GCB)	s.c./i.v.	Superior to rituximab
SU-DHL-6	DLBCL (GCB)	s.c.	Antitumoral efficacy
Raji	Burkitt's lymphoma	s.c./i.v.	Antitumoral efficacy
OCI-LY3	DLBCL (ABC)	s.c.	No tumor engraftment

fNHL, follicular non-Hodgkin's lymphoma; i.v., intravenous; s.c., subcutaneous.

100 mg kg^{-1} inhibited the growth of RL tumors and resulted in some complete tumor remissions. After discontinuation of the twice-weekly antibody treatment, both high-dose groups were eligible for an additional week observation period. Without further antibody treatment the growth of RL xenografts was delayed but regrowth could not be prevented. Rituximab was included at 30 mg kg^{-1} for direct comparison to obinutuzumab. The antitumor activity of rituximab was inferior (TGI 43%) to equivalent dosing of obinutuzumab (TGI 75%) [108].

Overall, obinutuzumab mediated statistically significant superior and dose-dependent, antitumoral efficacy in the SU-DHL-4, OCI LY 18, WSU DLCL2, Z138, and RL s.c. and disseminated xenograft models in direct comparison to rituximab; in the SU-DHL-6 and Raji s.c. or disseminated xenograft models, obinutuzumab mediated a strong dose-dependent, antitumoral efficacy (Table 62.2; F. Herting, T. Friess).

The mechanism behind the superior antitumor activity of obinutuzumab depending on the model likely involves both ADCC and ADCP (because of glycoengineering that leads to enhanced interaction with the muFcγRIV, the mouse homologous of the human hFcγRIIIa, expressed on murine effector cells) as well as to Type-II-related noneffector-cell-mediated activity (including direct cell death induction and/or reduced CD20 internalization). However, similar to rituximab where the *in vivo* mechanism of action is still poorly understood, the *in vivo* mechanism of action of obinutuzumab in xenograft models has not been fully elucidated. The *in vivo* xenograft studies reported here were performed in SCID beige or SCID mice in which muFcγRIV is expressed on monocytes, macrophages, and granulocytes, but not on NK cells. Of note, SCID beige mice have disabled NK cells and granulocytes, but functional monocytes and macrophages. Thus, it is possible that part of the superior *in vivo* activity of obinutuzumab compared to rituximab comes from effector cell populations, such as macrophages and monocytes. However, control experiments using a non-glycoengineered wild-type version of obinutuzumab suggest that the *in vivo* superiority of obinutuzumab in s.c. xenograft models does not depend on enhanced interactions of the glycoengineered Fc region with

murine effector cells but can be largely attributed to Type-II-related noneffector-cell-mediated activities. In humans, an additional contribution of enhanced ADCC mediated by NK cells can be expected as compared with mouse models.

Depending on the NHL xenograft model studied, consistent antitumor efficacy inducing regression of established tumors and/or complete tumor regression and long-term cures in NHL xenograft models was observed only for trough serum levels of approximately 60–600 $\mu g\,ml^{-1}$ corresponding to weekly doses of 10, 30, and 100 $mg\,kg^{-1}$. In general, obinutuzumab exhibited superior antitumor efficacy as compared to rituximab at the same dose when using doses of 30–60 $mg\,kg^{-1}$ once weekly, corresponding to trough levels of approximately 300–500 $\mu g\,ml^{-1}$ (T. Friess, C. Klein). These trough levels are comparable to the trough levels observed in Phase I and Phase II trials with obinutuzumab [109–113]. Taken together, these findings suggest that in order to take advantage of the superior efficacy of obinutuzumab in patients, exposure in a similar range to those identified in nonclinical xenograft models should achieved.

62.11 *In vivo* Activity of Obinutuzumab in Combination with Chemotherapy, Bcl-2, and MDM2 Inhibitors

In clinical practice, the combination of rituximab with chemotherapy results in a substantial clinical benefit. To assess the potential of chemotherapy combination, the efficacy of obinutuzumab in combination with bendamustine, fludarabine, and chlorambucil (Clb) was compared to the combination of the respective chemotherapy with rituximab and the respective monotherapies. Obinutuzumab plus bendamustine achieved superior TGI versus rituximab plus bendamustine and showed a statistically significant effect versus the respective single treatments. Similarly, combinations of obinutuzumab with fludarabine and Clb demonstrated significantly superior activity to rituximab-based treatment. Notably, in these preclinical studies, obinutuzumab plus chemotherapy was superior to the respective monotherapies and obinutuzumab monotherapy was at least as effective as rituximab plus chemotherapy *in vivo* [114]. Taken together, these data support further clinical investigation of obinutuzumab plus chemotherapy.

Bcl-2 plays an essential role during the development of B-cell malignancies. In order to investigate whether the mode of action of obinutuzumab is compatible with simultaneous inhibition of Bcl-2, combination studies using the Bcl-2, Bcl-xl cross-reactive inhibitors ABT-737 [115], ABT-273 [116], and the Bcl-2 selective inhibitor GDC-199 (ABT-199) [117–119] were performed in the SU-DHL4 model. The studies showed that obinutuzumab at suboptimal doses works together with Bcl-2 inhibition, resulting in strong antitumor activity including complete tumor remissions (F. Herting, T. Friess, D. Sampath, C. Klein). On the basis of these data, a Phase Ib clinical trial is currently ongoing evaluating the safety and efficacy of combining the Bcl-2 inhibitor GDC-199 with obinutuzumab in CLL patients (GP28331). Similarly, obinutuzumab showed combined activity with

MDM2 inhibitor inhibitors *in vitro* on CLL samples [47] and in the p53 wild-type xenograft model Z138 (F. Herting, C. Klein).

62.12 B-Cell Depletion by Obinutuzumab in Cynomolgus Monkeys

The efficacy of obinutuzumab at depleting B cells in cynomolgus monkeys was assessed in direct comparison to rituximab [8]. Obinutuzumab at 10 and 30 mg kg^{-1} was compared with rituximab at 10 mg kg^{-1} and vehicle following two i.v. doses administered on days 0 and 7. Peripheral blood B cells were reduced over 95% both with obinutuzumab and rituximab; however, lymph node B-cell numbers were only significantly decreased in obinutuzumab-treated animals with both dosing regimens; from day 9 onwards and on day 35 B cell numbers were still decreased by more than 90%. A dose-dependent effect was observed as obinutuzumab tested at 30 mg kg^{-1} appeared to lead to an enhanced level of depletion compared to 10 mg kg^{-1}. Taken together, obinutuzumab was more effective at depleting B cells from the lymph nodes of cynomolgus monkeys compared to rituximab [8]. In a second study, the effect of obinutuzumab on B-cell depletion in cynomolgus monkeys was compared with that of a non-glycoengineered wild-type version of obinutuzumab and rituximab (C. del Nagro). Obinutuzumab (30 mg kg^{-1}) was compared to non-glycoengineered wild-type obinutuzumab (30 mg kg^{-1}), rituximab (30 mg kg^{-1}), and vehicle following two IV doses administered on days 0 and 7. Peripheral blood B cells were reduced at early timepoints (days 2–23) in all treatment groups; however, the depth and duration of depletion observed was significantly greater with obinutuzumab and non-glycoengineered wild-type obinutuzumab-treated animals. Lymph node B-cell numbers were also reduced for all treatment groups at day 9, but only obinutuzumab and non-glycoengineered wild-type obinutuzumab-treated animals maintained significant B-cell reductions of more than 90% to day 51. Surprisingly, non-glycoengineered wild-type obinutuzumab-treated animals displayed the greatest magnitude of lymph node B-cell depletion; however, no statistical difference was found between either obinutuzumab variant. These results demonstrate that obinutuzumab as well as non-glycoengineered wild-type obinutuzumab possesses a greater capacity and durability for depleting B cells from both blood and lymph nodes of cynomolgus monkeys compared to rituximab, most likely due to the Type II character of obinutuzumab. The glycoengineering of the Fc part, although triggering enhanced ADCC, did not translate into a further enhanced B-cell depletion in the lymph nodes of cynomolgus monkeys (C. del Nagro).

To evaluate the functional impact that the increased extent of B-cell depletion with obinutuzumab versus rituximab has on the humoral immune response to foreign antigens, cynomolgus monkeys from the second study were immune challenged after treatment with either a naïve novel antigen that the animals had never experienced before (de novo response to tetanus toxoid) or with a booster immune rechallenge with an immunogen that the animals had already encountered prior

to CD20 antibody administration (memory-recall response to measles/rubella). These studies showed that the enhanced efficacy in terms of B-cell depletion of obinutuzumab translated into stronger suppression of de novo antibody responses, but left the protective humoral memory responses intact (C. del Nagro). The ability to block de novo humoral antibody responses may possibly be attributed to either the increased extent of endogenous B-cell depletion seen with obinutuzumab and/or the enhanced ability of obinutuzumab to deplete activated, CD20-expressing B cells. The lack of impact on memory-recall challenge speaks for the fact that antigen experienced, memory B cells do not any longer express CD20 [8].

62.13
Conclusion from Nonclinical Pharmacology Studies with Obinutuzumab

Nonclinical *in vitro* studies show that the novel glycoengineered Type II CD20 antibody obinutuzumab mediates superior induction of direct cell death and effector-cell-mediated ADCC and ADCP on a panel of NHL cell lines and in whole blood/peripheral blood mononucleated cells (PBMCs), whereas its potency to mediate CDC is significantly reduced compared to the two approved Type I CD20 antibodies rituximab and ofatumumab. In *ex vivo* autologous whole blood B-cell depletion studies with blood from healthy volunteers as well as CLL patients, obinutuzumab mediates superior B-cell depletion.

These superior properties of obinutuzumab translate into superior antitumor efficacy in direct comparison to rituximab against a number of aggressive s.c. and disseminated NHL xenograft models. Obinutuzumab was able to induce complete tumor remission and long-term survival (cure) and increased the overall survival in disseminated NHL xenograft models. The efficacious and optimal dose of obinutuzumab in xenograft models was in the range of 10–30 $mg\,kg^{-1}$ corresponding to trough serum levels of approximately 300–600 $\mu g\,ml^{-1}$. In addition, obinutuzumab worked together with classical chemotherapeutic agents including cyclophosphamide, chlorambucil (Clb), fludarabine, and bendamustine. Treatment with obinutuzumab also resulted in potent and superior depletion of B cells in peripheral blood and in lymphoid tissues of cynomolgus monkeys. Vaccination studies in cynomolgus monkeys showed that the enhanced efficacy in terms of B-cell depletion by obinutuzumab translated into superior suppression of de novo antibody responses, but left the protective humoral memory responses intact.

The data generated to date imply that obinutuzumab represents a novel class of therapeutic CD20 antibody with outstanding and unique efficacy compared to classical Type I and non-ADCC-enhanced CD20 antibodies. On the basis of these nonclinical data, it can be anticipated that the combination of a Type II antibody character together with improved ADCC and ADCP potency exclusive to obinutuzumab might translate into superior clinical efficacy.

62.14
Clinical Experiences with Obinutuzumab

On the basis of nonclinical data, obinutuzumab is currently being studied in various Phase Ib/II/III clinical trials, including four pivotal trials in first-line CLL, DLBCL, and FL. Most of the ongoing studies compare obinutuzumab in combination with chemotherapy in direct comparison to rituximab with chemotherapy as current standard of care. One Phase III study also assesses the role of obinutuzumab in the treatment of rituximab-refractory patients in combination with bendamustine against bendamustine alone. Data from a variety of Phase I–III studies have become available recently and are presented here. Table 62.3 gives an overview of past and current clinical trials with obinutuzumab.

62.15
Early Clinical Experience with Obinutuzumab in B-Cell Lymphoma

62.15.1
BO20999 Phase 1

Obinutuzumab was tested in three separate Phase Ia clinical studies [120]. In the first Phase I study (first-in-man, BO20999 Phase I), the safety, efficacy, and pharmacokinetics (PK) of obinutuzumab was evaluated in 21 patients with heavily pretreated, relapsed, or refractory CD20(+) indolent lymphoma. Patients received obinutuzumab in a dose-escalating manner (three per cohort, range 50/100 to 1200/2000 mg) for 8×21 day cycles. The majority of adverse events (AEs) were grade 1 and 2 (114 of 132 total AEs). Seven patients reported a total of 18 grade 3 or 4 AEs. Infusion-related reactions (IRRs) were the most common AE, with most occurring during the first infusion and resolving with appropriate management. Three patients experienced grade 3 or 4 drug-related IRRs. The best overall response was 43%, with five complete responses (CRs) and four partial responses (PRs). Data from this study suggested that obinutuzumab was well tolerated and demonstrated encouraging activity in patients with previously treated NHL up to doses of 2000 mg (NCT00517530) [109].

62.15.2
BO21003 Phase I

In the second phase I study the safety, tolerability, PK, and antitumor activity of obinutuzumab as induction therapy followed by 2 years of maintenance was evaluated. Cohorts of three to six patients received obinutuzumab (200–2000 mg) intravenously weekly for 4 weeks. Patients with a complete or PR (or stable disease and clinical benefit) continued to receive obinutuzumab every 3 months, for a maximum of eight doses. Twenty-two patients with relapsed CD20-positive NHL or CLL with an indication for treatment and no therapy of higher priority were

Table 62.3 Overview about clinical trials with obinutuzumab as single agent and in combination therapy.

				Treatment			
	Study	***N***	**Patient population**	**Induction**	**Maintenance**	**Primary end point**	**Recruitment status**
Phase I	GAUGUIN (BO20999) [1]	34	Relapsed CD20+	GA101	—	Safety	Completed
	GAUSS (BO21003) [2]	22	Relapsed CD20+	GA101	GA101	Safety	Completed
	JO21900 (Japan) [3]	12	Relapsed, refractory CD20+	GA101	—	Safety	Completed
	GAUDI (BO21000) [4]	56	Relapsed FL	GA101 + CHOP or GA101 + FC	GA101	Safety	Completed
		81	First-line FL	GA101 + CHOP or GA101 + B	GA101	Safety	
	GALTON (GAO4779g)	41	First-line CLL	GA101 + FC or GA101 + B	—	Safety	Completed
	GP28331	64	Relapsed, refractory or first-line CLL	GA101 + GDC-0199	—	MTD + safety	Active
Phase II	GAUGUIN (BO20999)	100	Relapsed or refractory iNHL, aNHL, CLL	GA101	—	ORR	Completed
	GAUSS (BO21003) [5]	175	Relapsed or refractory iNHL	GA101 vs R	GA101 vs R	ORR	Completed
	GATHER (GAO4915g)	95	First-line DLBCL	GA101 + CHOP	—	ORR + CR	Active
	GAGE (GAO4768g)	80	First-line CLL	GA101 (1000 mg) vs GA101 (2000 mg)	—	ORR	Completed
Phase III	CLL11 (BO21004)[a] [6, 7]	781[b]	First-line CLL with comorbidities	Chlorambucil vs GA101 + chlorambucil vs R + chlorambucil	—	PFS	Completed
	GADOLIN (GAO4753g)	360	R-refractory iNHL	GA101 + B vs B	GA101 (in GA101 + B arm only)	PFS	Active
	GOYA (BO21005)[c]	1400	First-line DLBCL	GA101 + CHOP vs R + CHOP	—	PFS	Active
	GALLIUM (BO21223)[d]	1400	First-line iNHL	GA101 + chemo vs R + chemo	GA101 vs R	PFS in FL	Active

aNHL, aggressive-histology non-Hodgkin lymphoma; MTD, maximum tolerated dose.
[a]Trial conducted in collaboration with the Deutsche CLL Studiengruppe (DCLLSG).
[b]Plus six additional G-Clb patients in safety run-in8.
[c]Trial conducted in collaboration with the Fondazione Italiana Linfomi (FIL) study group.
[d]Trial conducted in collaboration with the UK National Cancer Research Institute (NCRI) and the German Low-grade Lymphoma Study Group (GLSG)/ Eastern German Study Group for Hematology and Oncology (OSHO).

enrolled. Patients received a median of four prior regimens; 86% had received at least one rituximab-containing regimen. No dose-limiting or unexpected AEs were observed. IRRs were most common (all grades, 73%; grade 3/4, 18%), followed by infection (32%), pyrexia (23%), neutropenia (23%), headache (18%), and nausea (18%). At end of induction, 5 (23%) patients achieved PRs and 12 (54%) had stable disease. Eight patients received maintenance; the best overall response was 32% (six PRs/one CR). Obinutuzumab induction and maintenance therapy was well tolerated with promising efficacy in this heterogeneous, highly pretreated population (NCT00576758) [110].

62.15.3
JO21900

In the third phase I study (JO21900) obinutuzumab was evaluated in Japanese patients with relapsed or refractory B-cell lymphoma. In this Phase I dose-escalating study patients, the primary end point was to characterize the safety of obinutuzumab in a Japanese population; secondary end points were efficacy, PK, and pharmacodynamics. Patients received up to nine doses of obinutuzumab with up to 52 weeks' follow-up. Most AEs were grade 1 or 2 IRRs, and 10 grade 3/4 AEs occurred. No dose-limiting toxicities were observed and the maximum tolerated dose was not identified. Out of 12 patients, 7 responded (end-of-treatment response rate 58%), with two CRs and five PRs. Responses were observed from low to high doses, and no dose–efficacy relationship was observed. B-cell depletion occurred in all patients after the first infusion and was maintained for the duration of treatment. Serum levels of obinutuzumab increased in a dose-dependent manner, although there was interpatient variability. This Phase I study demonstrated that obinutuzumab has an acceptable safety profile and that it offers encouraging activity in Japanese patients with relapsed/refractory B-cell lymphoma [111].

62.16
Phase Ib and II Experience with Obinutuzumab in B-Cell Lymphoma

62.16.1
BO20999 Randomized Phase II in Indolent B-Cell Lymphoma

The aforementioned Phase I study BO20999 with single-agent obinutuzumab was later amended to compare two doses of obinutuzumab in the Phase II part of the study. This was done separately for a cohort of patients with follicular lymphoma and aggressive lymphoma (MCL and DLBCL). The Phase II part evaluated the efficacy and safety of two doses of obinutuzumab in patients with relapsed/refractory indolent B-cell lymphoma. Patients were randomized to receive eight cycles of obinutuzumab as a flat dose of 400 mg on days 1 and 8 of cycle 1 and day 1 of cycles 2–8 (400/400) or 1600 mg on days 1 and 8 of cycle 1 and 800 mg on day 1 of cycles 2–8 (1600/800). Forty patients were enrolled, including

34 with follicular lymphoma; 38/40 patients had previously received rituximab and 22/40 were rituximab refractory. The overall response rate (ORR) at the end of treatment was 55% (95% CI, 32–76%) in the 1600/800 mg group (9% complete responders) and 17% (95% CI, 4–41%) in the 400/400 mg group (no complete responders). Five out of 10 rituximab-refractory patients had an end-of-treatment response in the 1600/800 mg group versus 1/12 in the 400/400 mg group. Median progression-free survival (PFS) was 11.9 months in the 1600/800 mg group (range 1.8–33.9+ months) and 6.0 months in the 400/400 mg group (range 1.0–33.9+ months). The most common AEs were IRRs, seen in 73% of patients, but only two patients had grade 3/4 IRRs (both 1600/800 mg). No IRRs were considered serious, and no patients withdrew for IRRs. It was therefore concluded that the 1600/800 mg dose schedule of obinutuzumab has encouraging activity with an acceptable safety profile in relapsed/refractory iNHL [112].

62.16.2 BO21003 Randomized Phase II in Indolent Lymphoma

Obinutuzumab single-arm clinical studies have demonstrated responses in patients with relapsed/refractory B-cell lymphoma, but no direct comparison with rituximab was available. The aim of this randomized Phase II trial was to compare efficacy and safety of monotherapy with obinutuzumab versus rituximab in patients with relapsed iNHL. Patients with relapsed iNHL requiring therapy who had demonstrated a prior response (CR/complete response unconfirmed (CRu) or PR) to a rituximab-containing regimen lasting ≥6 months were eligible for this study. A total of 175 pts (149 follicular (FL) and 26 nonfollicular iNHL) stratified by histology were randomized 1 : 1 to receive four weekly infusions (days 1, 8, 15, 22) of either obinutuzumab (1000 mg, $n = 87$) or rituximab (375 mg m^{-2}, $n = 88$). End-of-treatment response was assessed 28–42 days after the last induction dose. Patients without evidence of progression following induction therapy received ongoing treatment with obinutuzumab or rituximab every 2 months for up to 2 years at the same dose. The primary end point was ORR in the FL population. Secondary end points included PFS, overall survival (OS), and safety. Treatment arms were well balanced for standard prognostic features (age, ECOG PS, Ann Arbor stage, Follicular Lymphoma International Prognostic Index (FLIPI) risk score at initial diagnosis, lactate dehydrogenase (LDH)) and prior treatment characteristics. Patients in both arms had received a median of two prior lines of therapy (range: one to seven obinutuzumab arm; one to six rituximab arm) and 99% had received prior rituximab. At baseline, patients in the obinutuzumab cohort had a larger volume of disease based on the median sum of product diameters (SPDs): SPD obinutuzumab cohort 2397 mm^2 (range 192–29 326 mm^2) versus SPD rituximab cohort 1934 mm^2 (range 252–11 255 mm^2). The primary efficacy analysis was conducted in the FL population at the end of induction. On the basis of investigator assessment, ORR for obinutuzumab was 43.2% (32/74) versus 38.7% (29/75) for rituximab. The difference in response rates was 4.6% (95% CI [−12.0, 21.1]). The CR/CRu rate in the obinutuzumab arm was 10.8 versus 6.7% for rituximab. At the time of analysis,

28/149 patients had progressed, 15/74 on obinutuzumab, and 13/75 on rituximab. A central blinded radiology review (independent review facility, IRF) was performed to independently assess the response. The difference in response rates by the IRF was 15.2% (95% CI [−0.7, 31.2]; ORR, obinutuzumab vs rituximab: 43.2% [32/74] vs 28.0% [21/75]). In the overall population (FL + nonfollicular iNHL), the ORR as assessed by investigators was 43.2% (38/88) versus 35.6% (31/87) and by the IRF was 42.0% (37/88) versus 24.1% (21/87) for obinutuzumab and rituximab, respectively. Safety was analyzed in the overall population. No new safety signals were observed in either arm. One patient in the rituximab arm died from cardiopulmonary arrest and one patient in the obinutuzumab arm died from pulmonary aspergillosis. More patients discontinued therapy during induction in the rituximab arm (7 pts vs 4 obinutuzumab patients). Discontinuations with obinutuzumab occurred as a result of IRRs (3 pts) and orthostatic hypotension (1 pt). A greater number of patients in the rituximab arm experienced a serious adverse event (SAE) during the induction period (9 pts vs 5 obinutuzumab pts). SAEs in the obinutuzumab arm occurred as a result of IRR (2 pts), febrile neutropenia (1 pt), pleural effusion (1 pt), and nephrolithiasis (1 pt). More patients in the obinutuzumab arm reported IRRs (obinutuzumab vs rituximab: any grade, 72 vs 49%; grade 3/4, 11 vs 5%). IRRs were primarily seen during the first infusion and decreased in both frequency and severity with subsequent infusions. Other AEs (any grade) that occurred at a ≥5% higher incidence with obinutuzumab included fatigue (23 vs 17%), cough (10 vs 1%), back pain (7 vs 2%), decreased appetite (7 vs 2%), and insomnia (5 vs 0%). The conclusions were that treatment with obinutuzumab in patients with relapsed indolent B-cell lymphoma resulted in higher response rates compared to rituximab as assessed by both investigators and the IRF at an early time point. Obinutuzumab was well tolerated, although a higher rate of IRRs was noted; the majority were grade 1/2 in severity and did not result in significant differences in treatment discontinuation. This was the first head to head trial of obinutuzumab against rituximab and has demonstrated higher response rates without appreciable differences in safety. Further updates of this study are planned [121].

62.16.3 BO20999 Randomized Phase II in Aggressive B-Cell Lymphoma

As obinutuzumab was superior to rituximab in human DLBCL and MCL xenograft models and in Phase I of the current study, obinutuzumab exhibited encouraging activity but no clear dose–response relationship, it was considered appropriate to also study obinutuzumab in patients with aggressive histologies. The efficacy and safety of two doses of obinutuzumab were explored in this randomized Phase II trial in patients with heavily pretreated DLBCL and MCL. Patients were randomized to receive eight cycles of obinutuzumab either as a flat dose of 400 mg for all infusions (days 1 and 8 of cycle 1, day 1 of cycles 2–8) or 1600 mg on days 1 and 8 of cycle 1, and 800 mg on day 1 of cycles 2–8. Forty patients were enrolled – 21 in the 400/400 mg arm (10 DLBCL, 11 MCL) and 19 in the 1600/800 mg arm (15 DLBCL, 4 MCL). End-of-treatment response was 28% (32 and 24% in the

1600/800 and 400/400 mg arms, respectively). The best ORRs were 37 and 24%, respectively (DLBCL, 8/25 [32%]; MCL, 4/15 [27%]). Five of 25 (20%) rituximab-refractory patients responded, including 4/12 in the 1600/800 mg group. The most common AEs were IRRs, which were manageable. Three patients had grade 3/4 IRRs. Grade 3/4 neutropenia was seen in only one patient. In summary, and similar to the indolent part of the study, obinutuzumab 1600/800 mg was found to have encouraging PK and clinical activity with an acceptable safety profile in relapsed/refractory DLBCL and MCL, supporting further exploration [113].

62.16.4
BO21000 Randomized Phase II with Chemotherapy in Relapsed/Refractory Indolent B-Cell Lymphoma

The safety and activity of obinutuzumab plus chemotherapy in relapsed/refractory follicular lymphoma was explored in 56 patients. Participants received obinutuzumab plus cyclophosphamide, doxorubicin, vincristine, and prednisone (G-CHOP; every 3 weeks, six to eight cycles) or obinutuzumab plus fludarabine and cyclophosphamide (G-FC; every 4 weeks, four to six cycles). Patients were randomized to either obinutuzumab 1600 mg on days 1 and 8 of cycle 1 followed by 800 mg on day 1 of subsequent cycles or 400 mg for all doses. Treatment responders were eligible for obinutuzumab maintenance (three monthly). Grade 1/2 IRRs were the most common treatment-related AE (all grades: G-CHOP, 68%; G-FC, 82%). Grade 3/4 IRRs were rare (7%) and restricted to first infusion. All patients received the planned obinutuzumab dose. Neutropenia was the most common treatment-related hematologic AE for G-CHOP (43%) and G-FC (50%). At the end of induction, 96% (27/28; CR, 39% [11/28])) of patients receiving G-CHOP and 93% (26/28; CR, 50% [14/28]) receiving G-FC showed responses. G-CHOP or FC (fludarabine and cyclophosphamide) had an acceptable safety profile, with no new or unexpected AEs, but G-FC was associated with more AEs than G-CHOP. Obinutuzumab plus chemotherapy resulted in 93–96% response rates, supporting Phase III investigations [122].

62.16.5
BO21000 Randomized Phase II with Chemotherapy in Previously Untreated Indolent B-Cell Lymphoma

Obinutuzumab was also tested in previously untreated patients with indolent lymphoma in the GAUDI study. Obinutuzumab was tested in combination with cyclophosphamide, doxorubicin, vincristine, and prednisone (CHOP) or bendamustine in 81 patients aged >18 years, with treatment-naïve CD20+ grade 1–3b FL with at least one measurable lesion (longest diameter >1.5 cm by computed tomography (CT) scan). All patients received a flat dose of obinutuzumab (1000 mg on days 1 and 8 of cycle 1 and day 1 of subsequent cycles) combined with either six to eight cycles of CHOP (every 3 weeks) or four to six cycles of bendamustine (90 mg m^{-2} days 1 and 2 every 4 weeks) on a per center choice basis. Patients

achieving CR or PR were eligible to receive obinutuzumab maintenance therapy (1000 mg) every 3 months for 2 years or until progression. The primary objective was safety, and secondary objectives included ORR, CR rate, and PK. Response was assessed at the end of induction using International Working Group response criteria; unconfirmed CRs were classified as PRs. Forty patients received G-CHOP and 41 G-bendamustine. Baseline characteristics were similar for both groups: median age was 53.5 and 57 years; bone marrow involvement 53 and 49%; bulky disease (≥7 cm) 45 and 41%; median time from diagnosis was only 1.20 months for both groups, high-risk FLIPI status (3–5) 45 and 46%, and intermediate risk (FLIPI 2) 38 and 34%. Thirty-eight G-CHOP and 37 G-bendamustine patients completed all cycles of planned induction therapy. Three patients withdrew without any response assessment. In the G-CHOP arm, one withdrawal was due to obinutuzumab-associated IRR after cycle 1 and another patient was found to be ineligible and withdrawn after cycle 1. In the G-bendamustine arm one patient withdrew consent after cycle 2. Three other patients were withdrawn after interim response assessment, none for safety reasons (insufficient response in the G-bendamustine arm and administrative reasons for two in the G-CHOP arm). The most frequent AEs were IRRs (all grades: 58% G-CHOP; 59% G-bendamustine; grade 3/4: 5% G-CHOP; 10% G-bendamustine). No Grade 3/4 IRRs occurred after cycle 3. Grade 3/4 neutropenia was reported in 43% of patients in the G-CHOP arm and 29% of patients in the G-bendamustine arm during induction, resulting in delayed delivery of 7.0 and 4.8% of chemotherapy cycles. All delays but one were no longer than 2 weeks. Grade 3/4 infections occurred in 23% of patients receiving G-CHOP and 10% of patients receiving G-bendamustine. Approximately half of these were neutropenic infections or sepsis and all resolved with appropriate management. ORR at the end of the induction period was 95% (38/40) in the G-CHOP arm (CR rate 35%) and 92.7% (38/41) in the G-bendamustine arm (CR rate 39%). Serum obinutuzumab concentrations increased during the induction period and were similar for both regimens. Mean C_{max} was 300–600 μg ml^{-1} and C_{min} 100–300 μg ml^{-1}. Following the final administration, a decline in obinutuzumab serum concentration was seen that was similar for the two treatment combinations. In conclusion, efficacy and safety data for obinutuzumab combined with CHOP and bendamustine are encouraging for first-line treatment of patients with FL. On the basis of these promising results obinutuzumab is now being studied in combination with various chemotherapy regimens in a randomized Phase III study against the standard of care, rituximab-based immunochemotherapy [123].

62.17
Phase III Studies with Obinutuzumab in B-Cell Lymphoma

Ongoing studies evaluate the place for obinutuzumab in the treatment of previously untreated patients with indolent lymphoma (BO21223 GALLIUM), previously untreated DLBCL (BO21005 GOYA), and rituximab-refractory patients (GAO4753g

GADOLIN). GALLIUM and GOYA use obinutuzumab in conjunction with standard chemotherapy versus established regimens, such as R-CHOP. GADOLIN evaluates the role of obinutuzumab against bendamustine in a rituximab-refractory population. Results from these studies are expected in the second half of the decade.

62.18
Obinutuzumab in CLL: Early Experience and Ongoing Phase II Studies

GAUGUIN BO20999 also evaluated the safety and efficacy of obinutuzumab monotherapy in patients with relapsed/refractory CLL. In Phase I, 13 patients received obinutuzumab at doses ranging from 400 to 1200 mg (days 1 and 8 of cycle 1, day 1 of cycles 2–8). In Phase II, a flat dose of 1000 mg was administered to 20 patients (days 1, 8, and 15 of cycle 1, day 1 of cycles 2–8). The most common AE was IRRs (95–100% of Phase I/II participants), most of which were grade 1/2. Grade 3/4 neutropenia was reported in 10 patients in Phase I, with no clear relationship to dose, and 4 patients in Phase II. No patient died while on treatment. Regarding the primary efficacy end points, the end-of-treatment response in Phase I and II was 62 and 15%, respectively (all PRs), and best overall response was 62 and 30%, respectively. In Phase II, median PFS was 10.7 months, and median duration of response was 8.9 months. Obinutuzumab monotherapy is therefore considered very active and well tolerated in patients with heavily pretreated relapsed/refractory CLL [124]. Notably, obinutuzumab resulted in rapid and complete B-cell depletion in peripheral blood of CLL patients to an extent not seen with other CD20 antibodies. Ongoing studies evaluate the role of obinutuzumab in conjunction with standard chemotherapy (FC, bendamustine) and a higher dose of obinutuzumab 2000 versus 1000 mg, both in previously untreated patients with CLL.

62.19
Phase III Experience with Obinutuzumab: The CLL11 Trial

On the basis of positive Phase I/II experience with obinutuzumab in CLL, a Phase III study was designed and conducted in collaboration with the German CLL Study Group [125, 126]. Chemoimmunotherapy, such as FCR, is standard of care in young and physically fit patients with CLL. Development of similar therapies for older and less fit CLL patients is ongoing, but data from phase III trials are sparse. CLL11 is the largest trial to evaluate three treatments in previously untreated CLL patients with comorbidities: Chlorambucil (Clb) alone, obinutuzumab + Clb (GClb), and Rituximab + Clb (RClb). The trial read out in two stages and the final data from both stages have recently been reported [127]. Treatment-naïve CLL patients with a Cumulative Illness Rating Scale (CIRS) total score >6 and/or an estimated creatinine clearance (CrCl) <70 ml/min were eligible. Patients received Clb alone (0.5 mg/kg po d1, d15 q28 days, 6 cycles), GClb (100 mg iv d1, 900 mg

d2, 1000 mg d8, d15 of cycle 1, 1000 mg d1 cycles 2–6), or RClb (375 mg/m^2 iv d1 cycle 1, 500 mg/m^2 d1 cycles 2–6). Primary endpoint was investigator-assessed progression-free survival (PFS). The median age, CIRS score, and CrCl at baseline were 73 years, 8, and 61.1 ml/min for stage 1a (Clb vs GClb, 356 pts) and 73 years, 8, and 62.1 ml/min for stage 1b (Clb vs RClb, 351 pts, triggered by a different event rate). Treatment with obinutuzumab-chlorambucil or rituximab-chlorambucil as compared with chlorambucil monotherapy, increased response rates and prolonged progression-free survival (median progression-free survival, 26.7 months with obinutuzumab-chlorambucil vs 11.1 months with chlorambucil alone; hazard ratio for progression or death, 0.18; 95% confidence interval [CI], 0.13–0.24; $P < 0.001$; and 16.3 months with rituximab-chlorambucil vs 11.1 months with chlorambucil alone; hazard ratio, 0.44; 95% CI, 0.34–0.57; $P < 0.001$). Treatment with obinutuzumab-chlorambucil, as compared with chlorambucil alone, prolonged overall survival (hazard ratio for death, 0.41; 95% CI, 0.23 to 0.74; P = 0.002). Treatment with obinutuzumab-chlorambucil, as compared with rituximab-chlorambucil, resulted in prolongation of progression-free survival (hazard ratio, 0.39; 95% CI, 0.31–0.49; $P < 0.001$) and higher rates of complete response (20.7% vs 7.0%) and molecular response. Infusion-related reactions and neutropenia were more common with obinutuzumab-chlorambucil than with rituximab-chlorambucil, but the risk of infection was not increased.

In conclusion, chemoimmunotherapy with obinutuzumab are superior over rituximab if both are added to chlorambucil.

Obinutuzumab in combination with chlorambucil has received orphan drug designation for the first-line therapy of CLL by FDA and EMA and based on the results of the CLL11 trial, obinutuzumab also received breakthrough therapy designation by FDA. On November 1, 2013 obinutuzumab was approved as first breakthrough therapy product based on the data of the stage 1a analysis of the CLL11 trial by the United States for the first-line treatment of CLL patients in combination with clorambucil under the tradename GAZYVA. Obinutuzumab in combination with chlorambucil has also been filed as a first-line therapy of CLL with the EMA and additional health authorities throughout the world.

References

1. Li, H., Ayer, L.M., Polyak, M.J., Mutch, C.M., Petrie, R.J., Gauthier, L., Shariat, N., Hendzel, M.J., Shaw, A.R., Patel, K.D. *et al.* (2004) The CD20 calcium channel is localized to microvilli and constitutively associated with membrane rafts: antibody binding increases the affinity of the association through an epitope-dependent cross-linking-independent mechanism. *J. Biol. Chem.*, **279** (19), 19893–19901.
2. Cartron, G., Watier, H., Golay, J., and Solal-Celigny, P. (2004) From the bench to the bedside: ways to improve rituximab efficacy. *Blood*, **104** (9), 2635–2642.
3. Maloney, D.G. (2012) Anti-CD20 antibody therapy for B-cell lymphomas. *N. Engl. J. Med.*, **366** (21), 2008–2016.
4. Okroj, M., Osterborg, A., and Blom, A.M. (2012) Effector mechanisms of anti-CD20 monoclonal antibodies in B cell malignancies. *Cancer Treat. Rev.*

5. Boross, P. and Leusen, J.H. (2012) Mechanisms of action of CD20 antibodies. *Am. J. Cancer Res.*, **2** (6), 676–690.
6. Weiner, G.J. (2010) Rituximab: mechanism of action. *Semin. Hematol.*, **47** (2), 115–123.
7. Abes, R., Gelize, E., Fridman, W.H., and Teillaud, J.L. (2010) Long-lasting antitumor protection by anti-CD20 antibody through cellular immune response. *Blood*, **116** (6), 926–934.
8. Mossner, E., Brunker, P., Moser, S., Puntener, U., Schmidt, C., Herter, S., Grau, R., Gerdes, C., Nopora, A., van Puijenbroek, E. *et al.* (2010) Increasing the efficacy of CD20 antibody therapy through the engineering of a new type II anti-CD20 antibody with enhanced direct and immune effector cell-mediated B-cell cytotoxicity. *Blood*, **115** (22), 4393–4302.
9. Glennie, M.J., French, R.R., Cragg, M.S., and Taylor, R.P. (2007) Mechanisms of killing by anti-CD20 monoclonal antibodies. *Mol. Immunol.*, **44** (16), 3823–3837.
10. Beers, S.A., Chan, C.H., French, R.R., Cragg, M.S., and Glennie, M.J. (2010) CD20 as a target for therapeutic type I and II monoclonal antibodies. *Semin. Hematol.*, **47** (2), 107–114.
11. Cragg, M.S. (2011) CD20 antibodies: doing the time warp. *Blood*, **118** (2), 219–220.
12. Illidge, T.M. (2012) Obinutuzumab (GA101)–a different anti-CD20 antibody with great expectations. *Expert Opin. Biol. Ther.*, **12** (5), 543–545.
13. Alduaij, W. and Illidge, T.M. (2011) The future of anti-CD20 monoclonal antibodies: are we making progress? *Blood*, **117** (11), 2993–3001.
14. Lim, S.H., Beers, S.A., French, R.R., Johnson, P.W., Glennie, M.J., and Cragg, M.S. (2010) Anti-CD20 monoclonal antibodies: historical and future perspectives. *Haematologica*, **95** (1), 135–143.
15. Weiner, G.J. (2010) Making a better antibody: all is not lost. *Blood*, **115** (25), 5127–5128.
16. Klein, C., Lammens, A., Schafer, W., Georges, G., Schwaiger, M., Mossner, E., Hopfner, K.P., Umana, P., and Niederfellner, G. (2013) Epitope interactions of monoclonal antibodies targeting CD20 and their relationship to functional properties. *MAbs*, **5** (1), 22–33.
17. Cragg, M.S., Morgan, S.M., Chan, H.T., Morgan, B.P., Filatov, A.V., Johnson, P.W., French, R.R., and Glennie, M.J. (2003) Complement-mediated lysis by anti-CD20 mAb correlates with segregation into lipid rafts. *Blood*, **101** (3), 1045–1052.
18. Chan, H.T., Hughes, D., French, R.R., Tutt, A.L., Walshe, C.A., Teeling, J.L., Glennie, M.J., and Cragg, M.S. (2003) CD20-induced lymphoma cell death is independent of both caspases and its redistribution into Triton X-100 insoluble membrane rafts. *Cancer Res.*, **63** (17), 5480–5489.
19. Niederfellner, G., Lammens, A., Mundigl, O., Georges, G.J., Schaefer, W., Schwaiger, M., Franke, A., Wiechmann, K., Jenewein, S., Slootstra, J.W. *et al.* (2011) Epitope characterization and crystal structure of GA101 provide insights into the molecular basis for type I/II distinction of CD20 antibodies. *Blood*, **118** (2), 358–367.
20. Alduaij, W., Ivanov, A., Honeychurch, J., Cheadle, E.J., Potluri, S., Lim, S.H., Shimada, K., Chan, C.H., Tutt, A., Beers, S.A. *et al.* (2011) Novel type II anti-CD20 monoclonal antibody (GA101) evokes homotypic adhesion and actin-dependent, lysosome-mediated cell death in B-cell malignancies. *Blood*, **117** (17), 4519–4529.
21. Honeychurch, J., Alduaij, W., Azizyan, M., Cheadle, E.J., Pelicano, H., Ivanov, A., Huang, P., Cragg, M.S., and Illidge, T.M. (2012) Antibody-induced nonapoptotic cell death in human lymphoma and leukemia cells is mediated through a novel reactive oxygen species-dependent pathway. *Blood*, **119** (15), 3523–3533.
22. Ivanov, A., Beers, S.A., Walshe, C.A., Honeychurch, J., Alduaij, W., Cox, K.L., Potter, K.N., Murray, S., Chan, C.H., Klymenko, T. *et al.* (2009) Monoclonal antibodies directed to CD20 and

HLA-DR can elicit homotypic adhesion followed by lysosome-mediated cell death in human lymphoma and leukemia cells. *J. Clin. Invest.*, **119** (8), 2143–2159.

23. Beers, S.A., French, R.R., Chan, H.T., Lim, S.H., Jarrett, T.C., Vidal, R.M., Wijayaweera, S.S., Dixon, S.V., Kim, H., Cox, K.L. *et al.* (2010) Antigenic modulation limits the efficacy of anti-CD20 antibodies: implications for antibody selection. *Blood*, **115** (25), 5191–5201.
24. Lim, S.H., Vaughan, A.T., Ashton-Key, M., Williams, E.L., Dixon, S.V., Chan, H.T., Beers, S.A., French, R.R., Cox, K.L., Davies, A.J. *et al.* (2011) Fc gamma receptor IIb on target B cells promotes rituximab internalization and reduces clinical efficacy. *Blood*, **118** (9), 2530–2540.
25. Poppema, S. and Visser, L. (1987) Preparation and application of monoclonal antibodies: B cell panel and parafin tissue reactive panel. *Biotest Bull.*, **3**, 131–139.
26. Stanfield, R.L., Zemla, A., Wilson, I.A., and Rupp, B. (2006) Antibody elbow angles are influenced by their light chain class. *J. Mol. Biol.*, **357** (5), 1566–1574.
27. Herter S, Herting F, Mundigl O, Waldhauer I, Weinzierl T, Fauti T, Muth G, Ziegler-Landesberger D, Van Puijenbroek E, Lang S, *et al.* Preclinical activity of the type II CD20 antibody GA101 (obinutuzumab) compared with rituximab and ofatumumab in vitro and in xenograft models. *Mol. Cancer Ther.* 2013, **12**, 2031–2042.
28. Du, J., Wang, H., Zhong, C., Peng, B., Zhang, M., Li, B., Huo, S., Guo, Y., and Ding, J. (2007) Structural basis for recognition of CD20 by therapeutic antibody Rituximab. *J. Biol. Chem.*, **282** (20), 15073–15080.
29. Teeling, J.L., Mackus, W.J., Wiegman, L.J., van den Brakel, J.H., Beers, S.A., French, R.R., van Meerten, T., Ebeling, S., Vink, T., Slootstra, J.W. *et al.* (2006) The biological activity of human CD20 monoclonal antibodies is linked to unique epitopes on CD20. *J. Immunol.*, **177** (1), 362–371.
30. Binder, M., Otto, F., Mertelsmann, R., Veelken, H., and Trepel, M. (2006) The epitope recognized by rituximab. *Blood*, **108** (6), 1975–1978.
31. Kern, D.J., James, B.R., Blackwell, S., Gassner, C., Klein, C., and Weiner, G.J. (2013) GA101 induces NK-cell activation and antibody-dependent cellular cytotoxicity more effectively than rituximab when complement is present. *Leuk. Lymphoma*, **54**, 2500–2505.
32. Wang, S.Y., Veeramani, S., Racila, E., Cagley, J., Fritzinger, D.C., Vogel, C.W., St John, W., and Weiner, G.J. (2009) Depletion of the C3 component of complement enhances the ability of rituximab-coated target cells to activate human NK cells and improves the efficacy of monoclonal antibody therapy in an in vivo model. *Blood*, **114** (26), 5322–30.
33. Tedder, T.F., Boyd, A.W., Freedman, A.S., Nadler, L.M., and Schlossman, S.F. (1985) The B cell surface molecule B1 is functionally linked with B cell activation and differentiation. *J. Immunol.*, **135** (2), 973–979.
34. Tedder, T.F. and Engel, P. (1994) CD20: a regulator of cell-cycle progression of B lymphocytes. *Immunol. Today*, **15** (9), 450–454.
35. Zhang, N., Khawli, L.A., Hu, P., and Epstein, A.L. (2005) Generation of rituximab polymer may cause hyper-cross-linking-induced apoptosis in non-Hodgkin's lymphomas. *Clin. Cancer Res.*, **11** (16), 5971–5980.
36. Shan, D., Ledbetter, J.A., and Press, O.W. (2000) Signaling events involved in anti-CD20-induced apoptosis of malignant human B cells. *Cancer Immunol. Immunother.*, **48** (12), 673–683.
37. Shan, D., Ledbetter, J.A., and Press, O.W. (1998) Apoptosis of malignant human B cells by ligation of CD20 with monoclonal antibodies. *Blood*, **91** (5), 1644–1652.
38. Byrd, J.C., Kitada, S., Flinn, I.W., Aron, J.L., Pearson, M., Lucas, D., and Reed, J.C. (2002) The mechanism of tumor cell clearance by rituximab in vivo in patients with B-cell chronic lymphocytic leukemia: evidence of caspase

activation and apoptosis induction. *Blood*, **99** (3), 1038–1043.

39. Jazirehi, A.R. and Bonavida, B. (2005) Cellular and molecular signal transduction pathways modulated by rituximab (rituxan, anti-CD20 mAb) in non-Hodgkin's lymphoma: implications in chemosensitization and therapeutic intervention. *Oncogene*, **24** (13), 2121–2143.
40. Deans, J.P., Li, H., and Polyak, M.J. (2002) CD20-mediated apoptosis: signalling through lipid rafts. *Immunology*, **107** (2), 176–182.
41. Daniels, I., Turzanski, J., and Haynes, A.P. (2008) A requirement for calcium in the caspase-independent killing of Burkitt lymphoma cell lines by Rituximab. *Br. J. Haematol.*, **142** (3), 394–403.
42. Daniels, I., Abulayha, A.M., Thomson, B.J., and Haynes, A.P. (2006) Caspase-independent killing of Burkitt lymphoma cell lines by rituximab. *Apoptosis*, **11** (6), 1013–1023.
43. Stanglmaier, M., Reis, S., and Hallek, M. (2004) Rituximab and alemtuzumab induce a nonclassic, caspase-independent apoptotic pathway in B-lymphoid cell lines and in chronic lymphocytic leukemia cells. *Ann. Hematol.*, **83** (10), 634–645.
44. Ghetie, M.A., Bright, H., and Vitetta, E.S. (2001) Homodimers but not monomers of Rituxan (chimeric anti-CD20) induce apoptosis in human B-lymphoma cells and synergize with a chemotherapeutic agent and an immunotoxin. *Blood*, **97** (5), 1392–1398.
45. Liu, Y., Zheng, M., Lai, Z., Xiong, D., Fan, D., Xu, Y., Peng, H., Shao, X., Yang, M., Wang, J. *et al.* (2004) Inhibition of human B-cell lymphoma by an anti-CD20 antibody and its chimeric F(ab′)2 fragment via induction of apoptosis. *Cancer Lett.*, **205** (2), 143–153.
46. van der Kolk, L.E., Evers, L.M., Omene, C., Lens, S.M., Lederman, S., van Lier, R.A., van Oers, M.H., and Eldering, E. (2002) CD20-induced B cell death can bypass mitochondria and caspase activation. *Leukemia*, **16** (9), 1735–1744.
47. Jak, M., van Bochove, G.G., van Lier, R.A., Eldering, E., and van Oers, M.H. (2011) CD40 stimulation sensitizes CLL cells to rituximab-induced cell death. *Leukemia*, **25** (6), 968–978.
48. Liu, Y.X., Xiong, D.S., Fan, D.M., Xu, Y.F., and Yang, C.Z. (2004) Apoptosis of Raji cells by an anti-CD20 antibody HI47 and its fragments. *Leuk. Res.*, **28** (2), 209–211.
49. Nagy, Z.A., Hubner, B., Lohning, C., Rauchenberger, R., Reiffert, S., Thomassen-Wolf, E., Zahn, S., Leyer, S., Schier, E.M., Zahradnik, A. *et al.* (2002) Fully human, HLA-DR-specific monoclonal antibodies efficiently induce programmed death of malignant lymphoid cells. *Nat. Med.*, **8** (8), 801–807.
50. Johansson, U., Higginbottom, K., and Londei, M. (2004) CD47 ligation induces a rapid caspase-independent apoptosis-like cell death in human monocytes and dendritic cells. *Scand J. Immunol.*, **59** (1), 40–49.
51. Mateo, V., Brown, E.J., Biron, G., Rubio, M., Fischer, A., Deist, F.L., and Sarfati, M. (2002) Mechanisms of CD47-induced caspase-independent cell death in normal and leukemic cells: link between phosphatidylserine exposure and cytoskeleton organization. *Blood*, **100** (8), 2882–2890.
52. Krause, G., Patz, M., Isaeva, P., Wigger, M., Baki, I., Vondey, V., Kerwien, S., Kuckertz, M., Brinker, R., Claasen, J. *et al.* (2012) Action of novel CD37 antibodies on chronic lymphocytic leukemia cells. *Leukemia*, **26** (3), 546–549.
53. Heider, K.H., Kiefer, K., Zenz, T., Volden, M., Stilgenbauer, S., Ostermann, E., Baum, A., Lamche, H., Kupcu, Z., Jacobi, A. *et al.* (2011) A novel Fc-engineered monoclonal antibody to CD37 with enhanced ADCC and high proapoptotic activity for treatment of B-cell malignancies. *Blood*, **118** (15), 4159–4168.
54. Krisanaprakornkit, S., Chotjumlong, P., Pata, S., Chruewkamlow, N., Reutrakul, V., and Kasinrerk, W. (2013) CD99 ligation induces intercellular cell adhesion molecule-1 expression and secretion in

human gingival fibroblasts. *Arch. Oral Biol.*, **58** (1), 82–93.

55. Cerisano, V., Aalto, Y., Perdichizzi, S., Bernard, G., Manara, M.C., Benini, S., Cenacchi, G., Preda, P., Lattanzi, G., Nagy, B. *et al.* (2004) Molecular mechanisms of CD99-induced caspase-independent cell death and cell-cell adhesion in Ewing's sarcoma cells: actin and zyxin as key intracellular mediators. *Oncogene*, **23** (33), 5664–5674.
56. Sohn, H.W., Choi, E.Y., Kim, S.H., Lee, I.S., Chung, D.H., Sung, U.A., Hwang, D.H., Cho, S.S., Jun, B.H., Jang, J.J. *et al.* (1998) Engagement of CD99 induces apoptosis through a calcineurin-independent pathway in Ewing's sarcoma cells. *Am. J. Pathol.*, **153** (6), 1937–1945.
57. Cardarelli, P.M., Quinn, M., Buckman, D., Fang, Y., Colcher, D., King, D.J., Bebbington, C., and Yarranton, G. (2002) Binding to CD20 by anti-B1 antibody or F(ab′)(2) is sufficient for induction of apoptosis in B-cell lines. *Cancer Immunol. Immunother.*, **51** (1), 15–24.
58. Golay, J. and Introna, M. (2012) Mechanism of action of therapeutic monoclonal antibodies: promises and pitfalls of in vitro and in vivo assays. *Arch Biochem. Biophys.*, **526** (2), 146–153.
59. Golay, J., Bologna, L., Andre, P.A., Buchegger, F., Mach, J.P., Boumsell, L., and Introna, M. (2010) Possible misinterpretation of the mode of action of therapeutic antibodies in vitro: homotypic adhesion and flow cytometry result in artefactual direct cell death. *Blood*, **116** (17), 3372–3373; author reply 3373–3374.
60. Cragg, M.S., Alduaij, W., Klein, C., Umana, P., Glennie, M.J., and Illidge, T.M. (2010) Novel lysosomal-dependent cell death following homotypic adhesion occurs within cell aggregates. *Blood*, **116** (17), 3373–3374.
61. Hallaert, D.Y., Jaspers, A., van Noesel, C.J., van Oers, M.H., Kater, A.P., and Eldering, E. (2008) c-Abl kinase inhibitors overcome CD40-mediated drug resistance in CLL: implications for therapeutic targeting of chemoresistant niches. *Blood*, **112** (13), 5141–5149.
62. Jak, M., van Bochove, G.G., Reits, E.A., Kallemeijn, W.W., Tromp, J.M., Umana, P., Klein, C., van Lier, R.A., van Oers, M.H., and Eldering, E. (2011) CD40 stimulation sensitizes CLL cells to lysosomal cell death induction by type II anti-CD20 mAb GA101. *Blood*, **118** (19), 5178–5188.
63. Cheadle, E.J., Sidon, L., Dovedi, S.J., Melis, M.H., Alduaij, W., Illidge, T.M., and Honeychurch, J. (2013) The induction of immunogenic cell death by type II anti-CD20 monoclonal antibodies has mechanistic differences compared with type I rituximab. *Br. J. Haematol.*, **162**, 842–845.
64. Hogarth, P.M. and Pietersz, G.A. (2012) Fc receptor-targeted therapies for the treatment of inflammation, cancer and beyond. *Nat. Rev. Drug Discov.*, **11** (4), 311–331.
65. Bruhns, P., Iannascoli, B., England, P., Mancardi, D.A., Fernandez, N., Jorieux, S., and Daeron, M. (2009) Specificity and affinity of human Fcgamma receptors and their polymorphic variants for human IgG subclasses. *Blood*, **113** (16), 3716–3725.
66. Nimmerjahn, F. and Ravetch, J.V. (2008) Fcgamma receptors as regulators of immune responses. *Nat. Rev. Immunol.*, **8** (1), 34–47.
67. Jefferis, R. (2009) Recombinant antibody therapeutics: the impact of glycosylation on mechanisms of action. *Trends Pharmacol. Sci.*, **30** (7), 356–362.
68. Radaev, S., Motyka, S., Fridman, W.H., Sautes-Fridman, C., and Sun, P.D. (2001) The structure of a human type III Fcgamma receptor in complex with Fc. *J. Biol. Chem.*, **276** (19), 16469–16477.
69. Sondermann, P., Huber, R., Oosthuizen, V., and Jacob, U. (2000) The 3.2-A crystal structure of the human IgG1 Fc fragment-Fc gammaRIII complex. *Nature*, **406** (6793), 267–273.
70. Ferrara, C., Grau, S., Jager, C., Sondermann, P., Brunker, P., Waldhauer, I., Hennig, M., Ruf, A., Rufer, A.C., Stihle, M. *et al.* (2011)

Unique carbohydrate-carbohydrate interactions are required for high affinity binding between FcgammaRIII and antibodies lacking core fucose. *Proc. Natl. Acad. Sci. U.S.A.*, **108** (31), 12669–12674.

71. Krapp, S., Mimura, Y., Jefferis, R., Huber, R., and Sondermann, P. (2003) Structural analysis of human IgG-Fc glycoforms reveals a correlation between glycosylation and structural integrity. *J. Mol. Biol.*, **325** (5), 979–989.
72. Sondermann, P. and Oosthuizen, V. (2002) X-ray crystallographic studies of IgG-Fc gamma receptor interactions. *Biochem. Soc. Trans.*, **30** (4), 481–486.
73. Mimura, Y., Ghirlando, R., Sondermann, P., Lund, J., and Jefferis, R. (2001) The molecular specificity of IgG-Fc interactions with Fc gamma receptors. *Adv. Exp. Med. Biol.*, **495**, 49–53.
74. Sondermann, P., Kaiser, J., and Jacob, U. (2001) Molecular basis for immune complex recognition: a comparison of Fc-receptor structures. *J. Mol. Biol.*, **309** (3), 737–749.
75. Sondermann, P., Huber, R., and Jacob, U. (1999) Crystal structure of the soluble form of the human Fcgamma-receptor IIb: a new member of the immunoglobulin superfamily at 1.7 A resolution. *Embo J.*, **18** (5), 1095–1103.
76. Jefferis, R. and Lund, J. (2002) Interaction sites on human IgG-Fc for FcgammaR: current models. *Immunol. Lett.*, **82** (1-2), 57–65.
77. Shields, R.L., Lai, J., Keck, R., O'Connell, L.Y., Hong, K., Meng, Y.G., Weikert, S.H., and Presta, L.G. (2002) Lack of fucose on human IgG1 N-linked oligosaccharide improves binding to human Fcgamma RIII and antibody-dependent cellular toxicity. *J. Biol. Chem.*, **277** (30), 26733–26740.
78. Umana, P., Jean-Mairet, J., Moudry, R., Amstutz, H., and Bailey, J.E. (1999) Engineered glycoforms of an antineuroblastoma IgG1 with optimized antibody-dependent cellular cytotoxic activity. *Nat. Biotechnol.*, **17** (2), 176–180.
79. Ferrara, C., Brunker, P., Suter, T., Moser, S., Puntener, U., and Umana, P. (2006) Modulation of therapeutic antibody effector functions by glycosylation engineering: influence of Golgi enzyme localization domain and co-expression of heterologous beta1, 4-N-acetylglucosaminyltransferase III and Golgi alpha-mannosidase II. *Biotechnol. Bioeng.*, **93** (5), 851–61.
80. Ashraf, S.Q., Umana, P., Mossner, E., Ntouroupi, T., Brunker, P., Schmidt, C., Wilding, J.L., Mortensen, N.J., and Bodmer, W.F. (2009) Humanised IgG1 antibody variants targeting membrane-bound carcinoembryonic antigen by antibody-dependent cellular cytotoxicity and phagocytosis. *Br. J. Cancer*, **101** (10), 1758–1768.
81. Schuster, M., Umana, P., Ferrara, C., Brunker, P., Gerdes, C., Waxenecker, G., Wiederkum, S., Schwager, C., Loibner, H., Himmler, G. *et al.* (2005) Improved effector functions of a therapeutic monoclonal Lewis Y-specific antibody by glycoform engineering. *Cancer Res.*, **65** (17), 7934–7941.
82. Mori, K., Iida, S., Yamane-Ohnuki, N., Kanda, Y., Kuni-Kamochi, R., Nakano, R., Imai-Nishiya, H., Okazaki, A., Shinkawa, T., Natsume, A. *et al.* (2007) Non-fucosylated therapeutic antibodies: the next generation of therapeutic antibodies. *Cytotechnology*, **55** (2-3), 109–114.
83. Yamane-Ohnuki, N. and Satoh, M. (2009) Production of therapeutic antibodies with controlled fucosylation. *MAbs*, **1** (3), 230–236.
84. Nimmerjahn, F. and Ravetch, J.V. (2005) Divergent immunoglobulin g subclass activity through selective Fc receptor binding. *Science*, **310** (5753), 1510–1512.
85. Shinkawa, T., Nakamura, K., Yamane, N., Shoji-Hosaka, E., Kanda, Y., Sakurada, M., Uchida, K., Anazawa, H., Satoh, M., Yamasaki, M. *et al.* (2003) The absence of fucose but not the presence of galactose or bisecting N-acetylglucosamine of human IgG1 complex-type oligosaccharides shows

the critical role of enhancing antibody-dependent cellular cytotoxicity. *J. Biol. Chem.*, **278** (5), 3466–3473.

86. Ferrara, C., Stuart, F., Sondermann, P., Brunker, P., and Umana, P. (2006) The carbohydrate at FcgammaRIIIa Asn-162. An element required for high affinity binding to non-fucosylated IgG glycoforms. *J. Biol. Chem.*, **281** (8), 5032–5036.

87. Ito, A., Ishida, T., Utsunomiya, A., Sato, F., Mori, F., Yano, H., Inagaki, A., Suzuki, S., Takino, H., Ri, M. *et al.* (2009) Defucosylated anti-CCR4 monoclonal antibody exerts potent ADCC against primary ATLL cells mediated by autologous human immune cells in NOD/Shi-scid, IL-2R gamma(null) mice in vivo. *J. Immunol.*, **183** (7), 4782–4791.

88. Ito, A., Ishida, T., Yano, H., Inagaki, A., Suzuki, S., Sato, F., Takino, H., Mori, F., Ri, M., Kusumoto, S. *et al.* (2009) Defucosylated anti-CCR4 monoclonal antibody exercises potent ADCC-mediated antitumor effect in the novel tumor-bearing humanized NOD/Shi-scid, IL-2Rgamma(null) mouse model. *Cancer Immunol. Immunother.*, **58** (8), 1195–1206.

89. Ishida, T., Joh, T., Uike, N., Yamamoto, K., Utsunomiya, A., Yoshida, S., Saburi, Y., Miyamoto, T., Takemoto, S., Suzushima, H. *et al.* (2012) Defucosylated anti-CCR4 monoclonal antibody (KW-0761) for relapsed adult T-cell leukemia-lymphoma: a multicenter phase II study. *J. Clin. Oncol.*, **30** (8), 837–842.

90. Suzuki, R. (2010) Dosing of a phase I study of KW-0761, an anti-CCR4 antibody, for adult T-cell leukemia-lymphoma and peripheral T-cell lymphoma. *J. Clin. Oncol.*, **28** (23), e404–e405; author reply e406.

91. Yamamoto, K., Utsunomiya, A., Tobinai, K., Tsukasaki, K., Uike, N., Uozumi, K., Yamaguchi, K., Yamada, Y., Hanada, S., Tamura, K. *et al.* (2010) Phase I study of KW-0761, a defucosylated humanized anti-CCR4 antibody, in relapsed patients with adult T-cell leukemia-lymphoma and peripheral T-cell lymphoma. *J. Clin. Oncol.*, **28** (9), 1591–1598.

92. Ishii, T., Ishida, T., Utsunomiya, A., Inagaki, A., Yano, H., Komatsu, H., Iida, S., Imada, K., Uchiyama, T., Akinaga, S. *et al.* (2010) Defucosylated humanized anti-CCR4 monoclonal antibody KW-0761 as a novel immunotherapeutic agent for adult T-cell leukemia/lymphoma. *Clin. Cancer Res.*, **16** (5), 1520–1531.

93. Beck, A. and Reichert, J.M. (2012) Marketing approval of mogamulizumab: a triumph for glyco-engineering. *MAbs*, **4** (4), 419–425.

94. Radaev, S. and Sun, P.D. (2001) Recognition of IgG by Fcgamma receptor. The role of Fc glycosylation and the binding of peptide inhibitors. *J. Biol. Chem.*, **276** (19), 16478–16483.

95. Nagarajan, S., Anderson, M., Ahmed, S.N., Sell, K.W., and Selvaraj, P. (1995) Purification and optimization of functional reconstitution on the surface of leukemic cell lines of GPI-anchored Fc gamma receptor III. *J. Immunol. Methods*, **184** (2), 241–251.

96. Peipp, M., Lammerts van Bueren, J.J., Schneider-Merck, T., Bleeker, W.W., Dechant, M., Beyer, T., Repp, R., van Berkel, P.H., Vink, T., van de Winkel, J.G. *et al.* (2008) Antibody fucosylation differentially impacts cytotoxicity mediated by NK and PMN effector cells. *Blood*, **112** (6), 2390–2399.

97. Golay, J., Bologna, L., Da Roit, F., Rambaldi, A., Klein, C., Introna, M. (2013) Glycoengineered afucosylated anti-CD20 antibodies activate neutrophils mediated phagocytosis but not ADCC more efficiently than rituximab, *Blood*, **122**, 3482–3491.

98. Braza, M.S., Klein, B., Fiol, G., and Rossi, J.F. (2011) Gammadelta T-cell killing of primary follicular lymphoma cells is dramatically potentiated by GA101, a type II glycoengineered anti-CD20 monoclonal antibody. *Haematologica*, **96** (3), 400–407.

99. Pievani, A., Belussi, C., Klein, C., Rambaldi, A., Golay, J., and Introna, M. (2011) Enhanced killing of human B-cell lymphoma targets by combined

use of cytokine-induced killer cell (CIK) cultures and anti-CD20 antibodies. *Blood*, **117** (2), 510–518.

100. Bologna, L., Gotti, E., Manganini, M., Rambaldi, A., Intermesoli, T., Introna, M., and Golay, J. (2011) Mechanism of action of type II, glycoengineered, anti-CD20 monoclonal antibody GA101 in B-chronic lymphocytic leukemia whole blood assays in comparison with rituximab and alemtuzumab. *J. Immunol.*, **186** (6), 3762–3769.

101. Herter, S., Birk, M.C., Klein, C., Gerdes, C.A., Umana, P., Bacac, M. (2014) Glycoengineering of therapeutic antibodies enhances monocyte/macrophage-mediated phagocytosis and cytotoxicity, *J. Immunology.*, **192** (5), 2252–2260.

102. Golay, J., Bologna, L., Da Roit, F., Rambaldi, A., Klein, C., Introna, M. (2013) Glycoengineered afucosylated anti-CD20 antibodies activate neutrophils mediated phagocytosis but not ADCC more efficiently than rituximab, *Blood*, **122**, 3482–3491.

103. Herter, S., Del Giudice, I., Schmidt, C., Fauti, T., Klein, C., Umana, P., Dyer, M.J.S., Foa, R., and Grau, R. (2009) The novel type II CD20 antibody GA101 mediates superior B cell depletion in whole blood from healthy volunteers and B-CLL patients. *Haematologica*, **94** (s2), 20, abstract 910.

104. Patz, M., Isaeva, P., Forcob, N., Muller, B., Frenzel, L.P., Wendtner, C.M., Klein, C., Umana, P., Hallek, M., and Krause, G. (2011) Comparison of the in vitro effects of the anti-CD20 antibodies rituximab and GA101 on chronic lymphocytic leukaemia cells. *Br. J. Haematol.*, **152** (3), 295–306.

105. Laprevotte, E., Ysebaert, L., Klein, C., Valleron, W., Blanc, A., Gross, E., Laurent, G., Fournie, J.J., and Quillet-Mary, A. (2013) Endogenous IL-8 acts as a CD16 co-activator for natural killer-mediated anti-CD20 B cell depletion in chronic lymphocytic leukemia. *Leuk. Res.*, **37** (4), 440–446.

106. Rafiq, S., Butchar, J.P., Cheney, C., Mo, X., Trotta, R., Caligiuri, M., Jarjoura, D., Tridandapani, S., Muthusamy, N., and Byrd, J.C. (2013) Comparative assessment of clinically utilized CD20-directed antibodies in chronic lymphocytic leukemia cells reveals divergent NK cell, monocyte, and macrophage properties. *Journal of immunology*, **190** (6), 2702–2711.

107. Ysebaert, L., Laprévotte, E., Klein, C., Laurent, G., Fournié, J.J., and Quillet-Mary, A. (2013) In vitro activity of GA101 (obinutuzumab) on primary CLL cells is not diminished by the presence of molecular prognostic factors for poor clinical outcome [abstract]. Proceedings of the 103rd Annual Meeting of the American Association for Cancer Research, Washington, DC, Philadelphia, PA, April 6–10, 2013, Abstract 2829.

108. Dalle, S., Reslan, L., Besseyre de Horts, T., Herveau, S., Herting, F., Plesa, A., Friess, T., Umana, P., Klein, C., and Dumontet, C. (2011) Preclinical studies on the mechanism of action and the anti-lymphoma activity of the novel anti-CD20 antibody GA101. *Mol. Cancer Ther.*, **10** (1), 178–185.

109. Salles, G., Morschhauser, F., Lamy, T., Milpied, N., Thieblemont, C., Tilly, H., Bieska, G., Asikanius, E., Carlile, D., Birkett, J. *et al.* (2012) Phase 1 study results of the type II glycoengineered humanized anti-CD20 monoclonal antibody obinutuzumab (GA101) in B-cell lymphoma patients. *Blood*, **119** (22), 5126–5132.

110. Sehn, L.H., Assouline, S.E., Stewart, D.A., Mangel, J., Gascoyne, R.D., Fine, G., Frances-Lasserre, S., Carlile, D.J., and Crump, M. (2012) A phase 1 study of obinutuzumab induction followed by 2 years of maintenance in patients with relapsed CD20-positive B-cell malignancies. *Blood*, **119** (22), 5118–5125.

111. Ogura, M., Tobinai, K., Hatake, K., Uchida, T., Suzuki, T., Kobayashi, Y., Mori, M., Terui, Y., Yokoyama, M., and Hotta, T. (2012) Phase I study of obinutuzumab (GA101) in Japanese patients with relapsed or refractory B-cell non-Hodgkin lymphoma. *Cancer Sci.*, **104** (1), 105–110.

112. Salles, G.A., Morschhauser, F., Solal-Celigny, P., Thieblemont, C., Lamy, T., Tilly, H., Gyan, E., Lei, G., Wenger, M., Wassner-Fritsch, E. *et al.* (2013) Obinutuzumab (GA101) in patients with relapsed/refractory indolent non-hodgkin lymphoma: results From the phase II GAUGUIN study. *J. Clin. Oncol.: Off. J. Am. Soc. Clin. Oncol.*, **31** (23), 2920–2926.
113. Morschhauser, F.A., Cartron, G., Thieblemont, C., Solal-Celigny, P., Haioun, C., Bouabdallah, R., Feugier, P., Bouabdallah, K., Asikanius, E., Lei, G. *et al.* (2013) Obinutuzumab (GA101) monotherapy in relapsed/refractory diffuse large B-cell lymphoma or mantle-cell lymphoma: results from the phase II GAUGUIN study. *J. Clin. Oncol. Off. J. Am. Soc. Clin. Oncol.*, **31**, 2912–2919.
114. Herting, F., Bader, S., Friess, T., Muth, G., Umana, P., and Klein, C. (2014) Enhanced antitumor activity of the glycoengineered Type II CD20 antibody obinutuzumab (GA101) in combination with chemotherapy in xenograft models of human lymphoma. *Leukemia & Lymphoma*, 1–26. [Epub ahead of print.]
115. Oltersdorf, T., Elmore, S.W., Shoemaker, A.R., Armstrong, R.C., Augeri, D.J., Belli, B.A., Bruncko, M., Deckwerth, T.L., Dinges, J., Hajduk, P.J. *et al.* (2005) An inhibitor of Bcl-2 family proteins induces regression of solid tumours. *Nature*, **435** (7042), 677–681.
116. Tse, C., Shoemaker, A.R., Adickes, J., Anderson, M.G., Chen, J., Jin, S., Johnson, E.F., Marsh, K.C., Mitten, M.J., Nimmer, P. *et al.* (2008) ABT-263: a potent and orally bioavailable Bcl-2 family inhibitor. *Cancer Res.*, **68** (9), 3421–3428.
117. Davids, M.S. and Letai, A. (2013) ABT-199: taking dead aim at BCL-2. *Cancer Cell*, **23** (2), 139–141.
118. Vandenberg, C.J. and Cory, S. (2013) ABT-199, a new Bcl-2-specific BH3 mimetic, has in vivo efficacy against aggressive Myc-driven mouse lymphomas without provoking thrombocytopenia. *Blood*, **121** (12), 2285–2288.
119. Souers, A.J., Leverson, J.D., Boghaert, E.R., Ackler, S.L., Catron, N.D., Chen, J., Dayton, B.D., Ding, H., Enschede, S.H., Fairbrother, W.J. *et al.* (2013) ABT-199, a potent and selective BCL-2 inhibitor, achieves antitumor activity while sparing platelets. *Nat. Med.*, **19** (2), 202–208.
120. van Oers, M.H. (2012) CD20 antibodies: type II to tango? *Blood*, **119** (22), 5061–5063.
121. Sehn, L.H., Goy, A., Offner, F.C., Martinelli, G., Friedberg, J., Lasserre, S.F., Fine, G., and Press, O.W. (2011) Randomized phase II trial comparing GA101 (Obinutuzumab) with rituximab in patients with relapsed CD20 indolent B-cell non-hodgkin lymphoma: preliminary analysis of the GAUSS study. ASH Annual Meeting Abstracts, 118, p. 269.
122. Radford, J., Davies, A., Cartron, G., Morschhauser, F., Salles, G., Marcus, R., Wenger, M., Lei, G., Wassner-Fritsch, E., and Vitolo, U. (2013) Obinutuzumab (GA101) plus CHOP or FC in relapsed/refractory follicular lymphoma: results of the GAUDI study (BO21000). *Blood*, **122**, 1137–1143.
123. Dyer, M.J.S., Grigg, A., Gonzalez, M., Dreyling, M., Rule, S.A., Lei, G., Wassner-Fritsch, E., Wenger, M.K., and Marlton, P. (2012) Obinutuzumab (GA101) in combination with cyclophosphamide, doxorubicin, vincristine and prednisone (CHOP) or bendamustine in patients with previously untreated Follicular Lymphoma (FL): results of the phase Ib GAUDI study (BO21000). ASH Annual Meeting Abstracts, Vol. 120, p. 3686.
124. Cartron, G., Morschhauser, F., Thieblemont, C., Lamy, T., Milpied, N., Tilly, H., Birkett, J., Salles, G., and Hallek, M. (2011) Results from a phase II study of obinutuzumab (GA101) monotherapy in relapsed/refractory chronic lymphocytic leukemia (CLL). *Haematologica* (EHA Annual Meeting Abstracts 0101), **96** (2 Suppl), 39–40.
125. Hallek, M. (2013) Chronic lymphocytic leukemia: 2013 update on diagnosis,

risk stratification and treatment. *Am. J. Hematol.*, **88**, 803–816.

126. Goede, V., Fischer, K., Busch, R., Jaeger, U., Dilhuydy, M.S., Wickham, N., De Guibert, S., Ritgen, M., Langerak, A.W., Bieska, G. *et al.* (2013) Chemoimmunotherapy with GA101 plus chlorambucil in patients with chronic lymphocytic leukemia and comorbidity: results of the CLL11 (BO21004) safety run-in. *Leukemia*, **27** (5), 1172–1174.

127. Goede, V., Fischer, K., Busch, R., Engelke, A., Eichhorst, B., Wendtner, C.M., Chagorova, T., de la Serna, J., Dilhuydy, M.-S., Illmer, T., et al. (2014) Obinutuzumab plus Chlorambucil in Patients with CLL and Coexisting Conditions. *N. Engl. J. Med.*, **370** 1101–1110.